https://doi.org/10.5194/tc-2020-293
Preprint. Discussion started: 19 October 2020

The Cryosphere Discussions

A method for solving heat transfer with phase change in ice or soil that allows for large time steps while guaranteeing energy conservation

Niccolò Tubini[1], Stephan Gruber[2], and Riccardo Rigon[1]

[1]Department of Civil, Environmental and Mechanical Engineering, Universtity of Trento, Trento, Italy
[2]Department of Geography and Environmental Studies, Carleton University, Ottawa, ON, K1S 5B6, Canada

Correspondence: Niccolò Tubini (niccolo.tubini@unitn.it)

Abstract. The accurate simulation of heat transfer with phase change is a central problem in cryosphere studies. This is because the nonlinear behaviour of enthalpy as function of temperature can prevent thermal models of snow, ice and frozen soil from converging to the correct solution. Existing numerical techniques rely on increased temporal resolution in trying to keep corresponding errors withing acceptable bounds. Here, we propose an algorithm, originally applied to solve water flow in soils, as a method to solve these integration issues with guaranteed convergence and conservation of energy for any time step size.

We review common modeling approaches, focusing on the fixed-grid method and on frozen soil. Based on this, we develop a conservative formulation of the governing equation and outline problems of alternative formulations in discretized form. Then, we apply the nested Newton-Casulli-Zanolli (NCZ) algorithm to a one-dimensional finite-volume discretization of the energy-enthalpy formulation.

Model performance is demonstrated against the Neumann and Lunardini analytical solutions and by comparing results from numerical experiments with integration time steps of one hour, one day, and ten days. Using our formulation and the NCZ algorithm, the convergence of the solver is guaranteed for any time step size. With this approach, the integration time step can be chosen to match the time scale of the processes investigated.

1 Introduction

Freezing and thawing of soils affect a wide range of biogeochemical and hydrological (Walvoord and Kurylyk, 2016; Schuur et al., 2015) processes and interact with engineered structures in cold regions. Correspondingly, the simulation of freezing and thawing soil is an important an well-researched topic (Streletskiy et al., 2019; Harris et al., 2009). Climate change brings additional urgency and new phenomena of interest to these studies. It is thus not a surprise that many models of freezing and

https://doi.org/10.5194/tc-2020-293
Preprint. Discussion started: 19 October 2020

thawing soil and ice exist, some of which are reviewed in Appendix A. Here, we propose a solution to a central challenge that these model have in common.

Published models can be categorized as empirical, analytical, or numerical (Riseborough et al., 2008). Empirical methods relate ground temperature or thawing/freezing depth (TFD) to simple topoclimatic factors (Zhang et al., 2008; Riseborough et al., 2008) and are relatively simple to apply. By contrast, analytical and numerical models are based on the conservation of mass and energy and can be divided in two broad groups (Tan et al., 2011). The first group focuses primarily on freezing and thawing, commonly known as the Stefan problem. The governing equation describes energy conservation with the heat flux modelled using the Fourier law. The second group considers the coupled problem of heat transfer and water flow in soils. In this case energy-entalphy conservation equation includes also the advective heat flux and it is coupled with the mass conservation equation. For both groups, the latent heat transfer during phase change of water leads to problems related to convergence, conservation, and restrictions to discretization of space and time (Bao et al., 2016).

Historically (Hu and Argyropoulos, 1996; Vuik, 1993), the first attempts to solve the problem of heat conduction considering the phenomena of solidification and melting date back to the studies by Lame and Clapeyron in 1831, and the analytical solutions presented by Stefan around 1890, and Neumann in 1921. Later, other analytical solutions were proposed in order to overcome some simplifications that were too restrictive (Zhang et al., 2008; Riseborough et al., 2008; Walvoord and Kurylyk, 2016). These analytical solutions, however, are limited to one dimensional problems and constrained in their initial and boundary conditions as well as the description of soil characteristics (Kurylyk et al., 2014a).

By contrast, numerical models can accommodate complex processes or configurations, including soil heterogeneities, complicated temperature boundary conditions, intermittent freeze-thaw and temporally variable thermal properties. Accurately representing phase transitions, however, is a non-trivial task and several different methods have been published. They can be broadly cast in two general groups: the so-called front-tracking methods and the fixed-grid methods (Voller et al., 1990). Even though this contribution is focused on modelling heat transfer in frozen soil or ice, the following review includes, and is relevant for, other fields of research that involve phase change.

Front-tracking methods are suitable whenever the two phases are divided by a spatially smooth and continuous front and thus the state of the system can be conveniently described by the position of this interface (Voller et al., 1990). The moving front is tracked defining a continuity ('Stefan') condition on the heat flux across it. For example, the one-dimensional model by Goodrich (1978; 1982) uses front-tracking in modelling frozen soil and the SICOPOLIS model (Greve, 1997a, b; Greve and Blatter, 2016) uses it to model polythermal ice sheets.

In frozen soil, however, a significant proportion of water can remain liquid at temperatures well below 0 °C. This depression of the melting temperature is due to the presence of solutes (Bouyoucos, 1913; Bouyoucos and McCool, 1915; Bouyoucos, 1920, 1923), surface effects in the interaction between water and soil particles as well as water and ice (Anderson and Tice, 1972; Clow, 2018), and the Gibbs-Thomson effect (Rempel et al., 2004; Watanabe and Mizoguchi, 2002). To some degree, also polycrystalline ice has a temperature-dependent liquid water content (Langham, 1974). The gradual phase change over a range of temperatures in soils is commonly described with the soil freezing characteristic curve (SFCC) (Kurylyk and Watanabe, 2013).

https://doi.org/10.5194/tc-2020-293
Preprint. Discussion started: 19 October 2020


The Cryosphere Discussions
Open Access
EGU

With phase change occurring over a range of temperatures, rather than at one specific temperature, front-tracking methods become computationally expensive (Voller et al., 1990) and conceptually ambiguous. This is the case in many industrial (Voller and Cross, 1981) and environmental problems. Additionally, front tracking is complicated because it requires either a deforming grid or a transformed coordinate system (Aschwanden and Blatter, 2009). By contrast, fixed-grid methods can accurately describing the thermodynamics of the problem without requiring additional complications in handling the computational domain. For these reasons, fixed-grid methods are generally preferable to front-tracking methods when simulating frozen soil.

Fixed-grid methods include the latent heat of fusion in their governing equation, avoiding the necessity to define a continuity condition across the moving boundary and related implementation problems. All contemporary fixed-grid methods we reviewed aim to solve the numerical integration using globally convergent algorithms (Appendix G). Three differing approaches for treating the latent heat of fusion exists: the enthalpy method, using a source term, and using apparent heat capacity. As analytical expressions, these methods look the same because their governing equations can be obtained from each other by the chain rule of derivation. As we will illustrate in the next section, problems can arise in the discrete domain where this rule is not always valid.

Here we present a numerical model of heat conduction with freezing and thawing in soils without water flow that guarantees exact energy conservation for any time step size and for a wide range of soil freezing characteristics. It is novel in using the nested Newton-Casulli-Zanolli (NCZ) algorithm (Casulli and Zanolli, 2010) for solving the nonlinear system obtained from discretizing the governing equation, written in terms of the specific enthalpy, using a semi-implicit finite volume scheme. The NCZ algorithm has previously been applied to solving water flow in soils and to our knowledge this is first application for solving the heat equation. Long time steps are desirable for example in applications related to permafrost thaw or hydrology.

The remainder of the paper is organized as follows. Section 2 reviews established approaches to study freezing and thawing phenomena in soils and points to relevant issues. Section 3 describes the new approach we propose. It details the discretization of the governing equation and the NCZ algorithm used to solve the resulting nonlinear numerical system. In Section 4, the new model is tested against analytical solutions and in Section 5, its performance is compared over a range of spatial and temporal resolutions. Section 6 summarises our findings and concludes this contribution. The Appendix B contains pseudocode to facilitate the implementation of the method we describe in other models.

2 The governing equation and their numerical issues

The governing equation of the problem in the first of the three approaches is written in terms of both the total enthalpy and temperature

$$\frac{\partial h(T)}{\partial t} = \nabla \cdot [\lambda(T) \nabla T] \tag{1}$$

where $h(T)$ is the specific enthalpy, T is temperature, $\lambda(T)$ is the thermal conductivity, and t is the time.

In the approach relying on apparent heat capacity, the governing equation is

$$C_a \frac{\partial T}{\partial t} = \nabla \cdot [\lambda(T) \nabla T] \tag{2}$$

https://doi.org/10.5194/tc-2020-293
Preprint. Discussion started: 19 October 2020

where

$$C_a = \frac{\partial h}{\partial T} = C_T + l_f \frac{\partial \theta_w}{\partial T} \tag{3}$$

is the apparent heat capacity that is the sum of the actual heat capacity C_T and a term representing the additional thermal capacity arising from phase change with the local derivative of the SFCC (Dall'Amico, 2010).

In the approach using a source term for latent heat, it is considered as a heat source

$$C_T \frac{\partial T}{\partial t} = \nabla \cdot [\lambda(T) \nabla T] - l_f \frac{\partial \theta_w}{\partial T} \,, \tag{4}$$

and in this equation, there are two unknowns: the temperature, and the liquid fraction θ_w appearing in the source term.

The specific enthalpy per unit mass is defined as

$$h = u + pv \tag{5}$$

where u is the specific internal energy, p is pressure, and v is the specific volume, the inverse of density. Assuming that the heat transfer occurs at constant pressure and volume the differential of the specific energy and of the specific enthalpy are equal (Appendix C). However, since the term enthalpy method is commonly used in the literature, we will refer to enthalpy instead of internal energy.

The specific enthalpy of a control volume of soil V_c can be calculated as the sum of the enthalpy of the soil particles, liquid water and ice (Dall'Amico et al., 2011):

$$h = h_{sp} + h_w + h_i \tag{6}$$

Defining a reference temperature T_{ref} the above terms becomes

$$\begin{aligned} h_{sp} &= \rho_{sp} c_{sp} (1 - \theta_s)(T - T_{ref}) \\ h_w &= \rho_w c_w \theta_w(T)(T - T_{ref}) + \rho_w l_f \theta_w(T) \\ h_i &= \rho_i c_i \theta_i(T)(T - T_{ref}) \end{aligned} \tag{7}$$

where l_f is the specific latent heat of fusion, ρ_{sp}, ρ_w and ρ_i are the densities of the soil particles, water, and ice, c_{sp}, c_w, c_i are the specif heat capacity of the soil particles, water, and ice, $\theta_w(T)$ is the unfrozen water content, and $\theta_i(T)$ is the ice content. The liquid water content and the ice content are evaluated using SFCCs (Dall'Amico et al., 2011) which are dependent on temperature and, in the general case, on temperature and water saturation. Usually the reference temperature, T_{ref}, is set to 273.15 K, the melting temperature of pure water at standard atmospheric pressure. By using Eq. (7) the enthalpy Eq. (6) can be rewritten as

$$h = C_T (T - T_{ref}) + \rho_w l_f \theta_w(T) \tag{8}$$

where $C_T = \rho_{sp} c_{sp} (1 - \theta_s) + \rho_w c_w \theta_w(T) + \rho_i c_i \theta_i(T)$ is the bulk heat capacity of the soil volume V_c.

https://doi.org/10.5194/tc-2020-293
Preprint. Discussion started: 19 October 2020

SFCCs have an inflection point (Bao et al., 2016) causing a sharp change in their derivative. This nonlinear behaviour gives rise to convergence problems during the solution of the system of equations resulting from the numerical approximation of the governing equation (Voller, 1990; Casulli and Zanolli, 2010). This is true for any method used such as finite differences (Westermann et al., 2016; Bao et al., 2016; Sergueev et al., 2003), finite elements (McKenzie et al., 2007), and finite volumes (Dall'Amico et al., 2011). As a consequence, the robustness (stability) of the numerics used is a fundamental and important issue in frozen soil models.

There is a more subtle aspect in the integration though. Analytically, Eq. (1, 2, and 4) are equivalent because Eq. (2 and 4) are derived from Eq. (1) by applying the chain rule of derivative on the enthalpy under the general assumption that the enthalpy is a differentiable variable. However, this is not necessarily so in the discrete domain where the derivative chain rule is not always valid. This is a known issue when dealing with hyperbolic equations (Roe, 1981), but often overlooked when treating the parabolic ones.

The apparent heat-capacity approach (Eq. 2) can suffer from large balance errors in the presence of high nonlinearities and strong gradients (Casulli and Zanolli, 2010). The key to deriving a conservative numerical method here concerns the discretization of the apparent heat capacity, and Nicolsky et al. (2007b) as well as Voller et al. (1990) discussed suitable techniques.

Referring to the work by Roe (Roe, 1981), it can be proven that, the discrete operator of C_a has to satisfy the requirement

$$\tilde{C}_{a_i}^{n+1/2}(T_i^{n+1} - T_i^n) = h(T_i^{n+1}) - h(T_i^n)\,, \tag{9}$$

ensuring preservation of the chain rule at the discrete level. Approximating the time derivative in Eq. (2) using a backward Euler scheme we obtain

$$\tilde{C}_{a_i}^{n+1/2}\frac{T_i^{n+1} - T_i^n}{\Delta t}\,, \tag{10}$$

and substituting the condition Eq. (9)

$$\frac{h(T_i^{n+1}) - h(T_i^n)}{T_i^{n+1} - T_i^n}\frac{T_i^{n+1} - T_i^n}{\Delta t} = \frac{h_i^{n+1} - h_i^n}{\Delta t} \tag{11}$$

This shows that solving Eq. (2) with a conservative numerical method, i.e. by making use of Eq. (9), is equivalent to solving the enthalpy formulation, Eq. (1). Roe's condition, however, is often not checked in numerical models.

The source-term approach presents problems analogous to those of the apparent heat-capacity formulation. Specifically, Eq. (4) is derived from Eq. (2) by moving the latent heat term to the right-hand-side of the equation. Equation (4) can be solved numerically using an iterative procedure (Voller et al., 1990) or the Decoupled Energy Conservation Parametrization method (DECP) (Zhang et al., 2008). As pointed out by Voller et al. 1990, the numerical solutions based on an iterative procedure may suffer from non-convergence problem unless under-relaxation is wisely applied, and additionally, it necessary to guarantee that the liquid fraction is in the range $(0, 1)$. With DECP, the energy equation is first solved without latent heat. Then, soil temperature and the liquid and solid fractions are readjusted to ensure energy conservation during phase change. This method is mainly used in land-surface models (LSMs) (Dai et al., 2003; Foley et al., 1996; Verseghy, 1991). In this case,

https://doi.org/10.5194/tc-2020-293
Preprint. Discussion started: 19 October 2020

Nicolsky et al. (2007a) showed that it results in an artificial stretch of the phase change region, with consequent inaccuracies in the simulation of active-layer thickness. A summary of relevant models is given in Table 1 and in Appendix A.

In summary, the governing equation can be written using three different approaches that are equivalent analytically, but not in their discrete formulation. Of the three, the enthalpy approach remains conservative, even when discretized, and should be preferred. An additional fundamental problem is the solution of the nonlinear system of equations. Current algorithms either require time step adaptation or may fail to converge, leading to unstable simulations and reduced computational efficiency (Casulli and Zanolli, 2010). Here we address this fundamental challenge by using the NCZ algorithm to solve the nonlinear system of equations. Compared to other algorithms, it guarantees convergence of the solution for any integration time step. When the time step is not constrained by numerical issues, it can be chosen to better match the time scale of the process under investigation.

3 A soil heat-transfer model using the NCZ algorithm

Frozen soil models are typically solved with time steps between seconds and hours. This may be motivated by the desire to resolve diurnal phenomena near the ground surface, and also, this often arises from limitations of the numerical schemes used. Many applications related to permafrost (Erum et al., 2019), on the other hand, only require the representation of seasonal and multi-annual variation, which can be accomplished using time steps of one or more days if permitted by the numerical schemes employed. In order to have a numerical scheme that does not suffer from time step restriction due to a stability condition, a semi-implicit time integration is required. A semi-implicit formulation includes the necessity of solving a nonlinear system of equations and the algorithm used for this is of great importance. Existing linearization algorithms such as the Picard or the Newton, require a sufficiently accurate initial guess. As reported by Casulli and Zanolli (2010) this can be obtained by using small time steps, often requiring an empirical criterion for time-step adaptation. Therefore, even if the numerical scheme does not require a time step restriction, one may still be required to solve the nonlinear system of equations. Moreover, to the knowledge of the authors and colleagues (F. Gugole, M. Dumbser, G. Stelling, personal communication, 2019), the currently used algorithms to solve nonlinear system do not offer a mathematically guaranteed convergence. This is important, because an inexact solution of the nonlinear system is not conservative (Casulli and Zanolli, 2010).

3.1 Discretization of the domain

The domain is partitioned using an unstructured orthogonal grid (Casulli and Walters, 2000), consisting of a set of nonoverlapping convex volumes Ω_i, $i = 1, 2, .., N_v$, separated by M internal faces Γ_j, $j = 1, 2, ..., M$. Let $\mathcal{A}_j$ denote the nonzero jth face area. Within each control volume a centre must be identified in such a way that the segment joining the centres of two adjacent volumes and the face shared by the two volumes have a nonempty intersection, are hortogonal to each other and have distance δ_j. Each control volume Ω_i may have an arbitrary number of faces. Let $\mathcal{F}_i$ denote the nonempty set of faces of the ith volume, with the exclusion of boundary faces. Moreover, let $\mathcal{P}(i, j)$ be the neighbour of volume i that shares face j with the ith control volume so that $1 \leq \mathcal{P}(i, j) \leq N_v$ for all $j \in \mathcal{F}_i$. The discrete variables h_i and T_i are located at centre of each element Ω_i. Using

https://doi.org/10.5194/tc-2020-293
Preprint. Discussion started: 19 October 2020

The Cryosphere Discussions
Open Access
EGU

Table 1. Summarizing table of relevant existing freezing models.

Model	Form	Time discretization	Nonlinear solver	Limitation
CLM	N. L. H[a]	Crank-Nicolson	Decoupled Energy Conservation Parametrization	Non-convergence problems associated with the DECP. Monotonicity time step restriction.
CoupModel	A. H. C[b].	Explicit	Not required	Stability time step restriction.
CryoGrid	A. H. C[b].	Implicit	Newton based algorithm	Convergence is not guaranteed[f].
GEOtop	A. H. C[b].	Implicit	Globally convergent Newton algorithm	Convergence is not guaranteed[f].
GIPL-2.0	E. F.[c]	Implicit	Newton algorithm with Godunov splitting	Convergence is not guaranteed[f].
Goodrich	N. L. H.[a]	Implicit	Front tacking method	Computationally expensive. Problems arise when the phase change occurs over a range of temperatures.
Hydrus 1D	A. H. C[b].	Implicit	Picard iteration	Convergence is not guaranteed[f].
MarsFlow	E. F.[c]	Implicit	Newton-Raphson algorithm	Convergence is not guaranteed[f].
NEST	S. T.[d]	Explicit	Not required	Stability time step restriction.
SoilVision	A. H. C[b].	Explicit & implicit	Newton-Raphson algorithm	Convergence is not guaranteed[f].
SUTRA	A. H. C[b].	Implicit	Picard iteration	Convergence is not guaranteed[f].
Crocus	E. F.[c]	Implicit	Decoupled Energy Conservation Parametrization	Non-convergence problems associated with the DECP.
SNOWPACK	S. T.[d]	Implicit	Not required	Non-convergence problems related to the source-sink term.
Aschwanden Blatter	E. G. M.[c]	Implicit	Newton based algorithm	Convergence is not guaranteed[f].
SICOPOLIS	N. L. H.[a]	Implicit	Front tracking method with a transformed coordinate system	Computationally expensive

[a]The governing equation is written in only in terms of temperature and the latent heat is not included. [b]Apparent heat capacity formulation. [c]Enthalpy formulation. [d]Source term formulation. [e]The heat flux is written in terms of enthalpy and not of temperature as in the enthalpy formulation. [f]There are no guarantees that the nonlinear solver converge.

a semi-implicit finite volume method, the discretization of Eq. (1) reads as

$$h_i(T_i^{n+1}) = h_i(T_i^n) + \Delta t \left[\sum_{j \in \mathcal{F}_i} \Lambda_j^{n+1} \frac{T_{\mathcal{P}(i,j)}^{n+1} - T_i^{n+1}}{\delta_j} + S_i^n \right] \tag{12}$$

https://doi.org/10.5194/tc-2020-293
Preprint. Discussion started: 19 October 2020

where Δt is the time step size,

$$\Lambda_j^{n+1} := \mathcal{A}_j \max\left[\lambda_i(T_i^n), \lambda_{\mathcal{P}(i,j)}(T^n_{\mathcal{P}(i,j)})\right] \tag{13}$$

and

$$S_i = \int_{\Omega_i} S \, d\Omega \tag{14}$$

is an optional source/sink term in volume, and $h_i(T)$ is the ith enthalpy given by

$$h_i(T) = \int_{\Omega_i} h(T) \, d\Omega. \tag{15}$$

Eq. (12) can be written in matrix form as

$$\boldsymbol{h}(\boldsymbol{T}) + \mathbf{A}\boldsymbol{T} = \boldsymbol{b} \tag{16}$$

where $\boldsymbol{T} = \{T_i\}$ is the vector of unknowns, $\boldsymbol{h}(\boldsymbol{T}) = h_i(T_i)$ is a vectorial function representing the discrete enthalpy, $\mathbf{A}$ is the energy flux matrix, and $\boldsymbol{b}$ is the right-hand-side vector of Eq. (12), which is properly augmented by the known Dirichlet boundary condition when necessary. For a given initial condition T_i^0, at any time step $n = 1, 2, \ldots$ Eq. (12) constitutes a nonlinear system for T_i^{n+1}, with the nonlinearity affecting only the diagonal of the system and being represented by the enthalpy $h_i(T_i^{n+1})$. This set of equations is a consistent and conservative discretization of Eq. (1). Therefore, regardless of the chosen spatial and temporal resolution, T_i^{n+1} is a conservative approximation of the new temperature.

3.2 Solution of the nonlinear system

Difficulties in solving the nonlinear system of Eq. (16) arise from the non-monotonic behaviour of the derivative of the enthalpy, $h(T)$, with respect to temperature. The NCZ algorithm used here was discovered by Casulli and Zanolli (2010) and overcomes these difficulties with a nested Newton algorithm, two subsequent Newton-type iterations. It is based on Jordan decomposition (Chistyakov, 1997) of the enthalpy function, rewriting it as the difference of two monotonic functions on which the Newton algorithm can be applied in a nested iteration. A mathematical proof of convergence exists for NCZ (Brugnano and Casulli, 2008, 2009; Casulli and Zanolli, 2010, 2012).

For each control volume the enthalpy function $h_i(T)$ can be defined as

$$h_i(T) = \int_{T_{ref}}^{T} C_{a,i}(\xi) d\xi \tag{17}$$

where $C_{a,i}(T)$ is is defined as $C_{a,i}(T) = \int_{\Omega_i} C_{a,i}(T) d\Omega$. $C_{a,i}(T)$ has to fulfil two requirements. The first one, C1, is that $C_{a,i}(T)$ is defined for every T and that it is a nonnegative function function with bounded variations. The second one, C2, is that there exist a T^* such that $C_{a,i}(T)$ is strictly positive and non decreasing in $(0, T^*)$ and nonincreasing in $(T^*, +\infty)$.

https://doi.org/10.5194/tc-2020-293
Preprint. Discussion started: 19 October 2020

Since $C_{a,i}(T)$ are nonnegative functions with bounded variations, they are almost everywhere differentiable, admit only discontinuities of the first kind, and can be expressed by using the Jordan decomposition (Fig.1) as the difference of two nonnegative, nondecreasing, and bounded functions:

$$\begin{aligned} p_i(T) &= C_{a,i}(T) & q_i(T) &= 0 & &\text{if } T \le T^* \\ p_i(T) &= C_{a,i}(T^*) & q_i(T) &= p_i(T) - C_{a,i}(T) & &\text{if } T > T^* \end{aligned} \tag{18}$$

Using Eq. (18) the enthalpy $h_i(T)$ can be written as $h_i(T) = h_{1,i}(T) - h_{2,i}(T)$ where:

$$\begin{aligned} h_{1,i}(T) &= h_i(T) & &\text{if } T \le T^* \\ h_{1,i}(T) &= h_i(T^*) + C_{a,i}(T^*)(T - T^*) & &\text{if } T > T^* \end{aligned}$$

$$\begin{aligned} h_{2,i}(T) &= 0 & &\text{if } T \le T^* \\ h_{2,i}(T) &= h_{1,i}(T) - h_i(T) & &\text{if } T > T^* \end{aligned} \tag{19}$$

By making use of Eq. (19) the algebraic system, Eq. (16), can be written as

$$\boldsymbol{h_1}(\boldsymbol{T}) - \boldsymbol{h_2}(\boldsymbol{T}) + \mathbf{A}\boldsymbol{T} = \boldsymbol{b} \tag{20}$$

and solved first by linearizing $\boldsymbol{h_2}$ with the NCZ algorithm as the outer iteration and then $\boldsymbol{h_1}$ as the inner iteration. The initial guess for the NCZ algorithm must be chosen such that $\boldsymbol{T}^0 \le \boldsymbol{T}^*$.

The most commonly used constitutive SFCCs (McKenzie et al., 2007; Kozlowski, 2007; Dall'Amico et al., 2011; Sheshukov and Nieber, 2011; Watanabe et al., 2011), used to define the enthalpy of frozen soil, satisfy the assumptions C1 and C2. In particular, the NCZ approach can be successfully applied to SFCCs models derived from the combination of existing SWRC models and the Clapeyron equation that in general are difficult to implement in numerical models based on the apparent heat capacity (Kurylyk and Watanabe, 2013). Functions describing the internal energy of other substances, for instance pure water (Andreas et al., 2005), satisfy the assumptions C1 and C2 and, therefore, the NCZ method can be successfully used to model phase change problems as it will be shown for the original Stefan problem, Sections (4.1, Appendix E).

4 Analytical Benchmarks

The numerical model is compared with the analytical solution presented by Neumann (cited in Kurylyk et al. (2014b)) for the problem of freezing water, i.e. the Stefan problem, and the three-zone analytical solution presented by Lunardini (1988).

4.1 Neumann analytical solution

Kurylyk et al. (2014b) recommended the Neumann solution due to its ability to represent differences between the thermal diffusivities of the thawed and frozen zones. Here we consider the freezing of pure water instead of soil since it is more

https://doi.org/10.5194/tc-2020-293
Preprint. Discussion started: 19 October 2020

The Cryosphere Discussions
Open Access
EGU

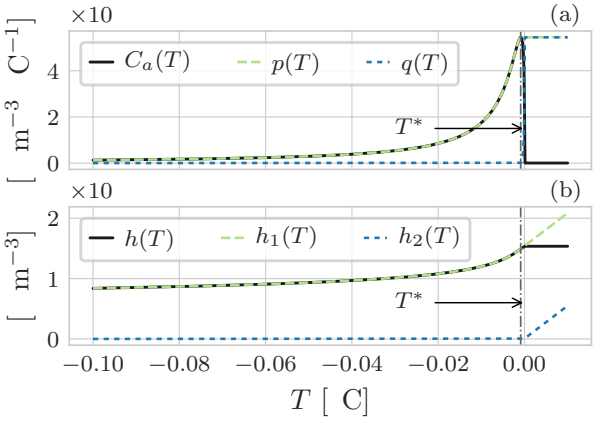

Figure 1. Graphical representation of the Jordan decomposition for the enthalpy of soil using the SFCC model for a silty soil (Dall'Amico, 2010). (a) shows the Jordan decomposition of $C_a(T)$, Eq. (18). For $T = T^*$, $C_a(T)$ presents a maximum: for $T < T^*$ it is increasing, and for $T > T^*$ it is decreasing. This non monothonic behaviour causes problems when solving the nonlinear system. $C_a(T)$ is thus replaced by $p(T)$ and $q(T)$, two monotonic functions. Consquently, (b), $h(T)$ is replaced by $h_1(T)$ and $h_2(T)$, Eq. (19)

numerically demanding. The domain is divided in two parts, the thawed and frozen zones, characterised by different thermal properties. Referring to the scheme in Fig. (2) the governing equations are

$$\frac{\partial h}{\partial t} = \lambda \frac{\partial^2 T}{\partial z^2} \tag{21}$$

$$T(\zeta, t) = T_m \tag{22}$$

$$\lambda_i \frac{\partial T}{\partial z}\bigg|_{z=\zeta^-} dt = \lambda_w \frac{\partial T}{\partial z}\bigg|_{z=\zeta^+} dt + l_f \rho \, d\zeta \tag{23}$$

At the moving boundary $\zeta(t)$, the temperature is equal to the melting temperature of water, and the time evolution of $\zeta(t)$ is described by the third equation, the Stefan condition. This condition states that the difference of the heat fluxes at the interface of the two substances is consumed for the phase change. The initial condition is $T(z,0) = T_0$ where $T_0 > T_m$, the surface boundary condition is $T(z=0,t) = T_s$, with $T_s < T_m$, and the bottom boundary condition is defined as $T(z \to \infty, t) = T_0$. The parameters used in the comparison are given in Table D1. The numerical model is able to simulate the freezing problem of water well as seen in Fig. (3) and Fig. (4).

For comparison, Kurylyk et al. 2014b tested the numerical model SUTRA against the Neumann analytical solution considering a soil porosity of $0.50\ \mathrm{m^3 m^{-3}}$. For their test the time step was of $0.04 - 0.4$ s, the vertical spatial discretization 0.001 m, and the parameter ϵ was increased to -0.01 °C to match the analytical solution. The maximum absolute error of the freezing front position was 0.00099 m.

In our model, the choice of a small melting temperature range $\epsilon = 0.0001$ °C does not affect the quality of the numerical solution even at a large time step of 3600 s. Looking at Table 2 it is clear that the choice of the time step size is somehow

https://doi.org/10.5194/tc-2020-293
Preprint. Discussion started: 19 October 2020

The Cryosphere
Discussions
Open Access
EGU

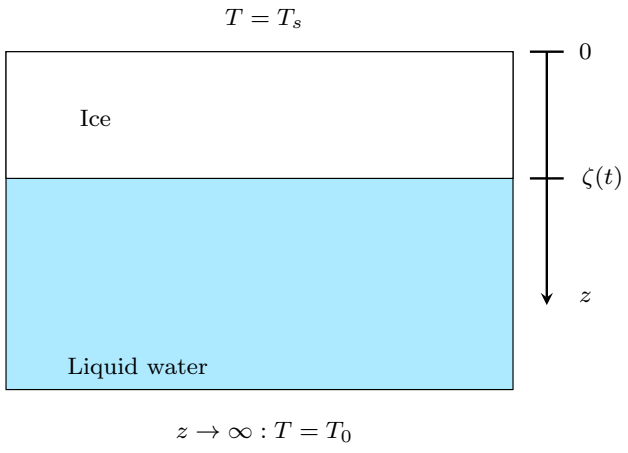

Figure 2. Scheme showing the setting of the Neumann solution for the freezing case. Initially water is liquid, $T_0 > T_m$. Because of the surface boundary condition, $T_s < T_m$, a freezing front, ζ, propagates downward.

Table 2. Maximum error m of the freezing front position from the numerical solution with the NCZ algorithm for different space and time discretizations relative to the Neumann analytical solution.

	$\Delta t = 60$ s	$\Delta t = 300$ s	$\Delta t = 3600$ s
$\Delta z = 0.001$ m	0.00737	0.00153	0.00739
$\Delta z = 0.005$ m	0.00271	0.00302	0.00714
$\Delta z = 0.01$ m	0.00536	0.00553	0.00905

related to the choice of the spatial discretization: using a small time step with a coarse grid does not necessarily improve the accuracy of the position of the freezing front. In Appendix E we report a comparison between the Neumann solution and the numerical solution for melting ice. Furthermore, Appendix G outlines the robustness of the NCZ algorithm in comparison with the Newton-Raphson and globally-convergent Newton methods. It has higher accuracy and tolerance for long time steps while avoiding the need for arbitrary additional parameters.

4.2 Lunardini analytical solution

Lunardini (1988) derived an analytical solution (Appendix F) for the temporal evolution of temperature during the freezing of a semi-infinite and initially unfrozen soil column. In contrast to the Neumann analytical solution, in the Lunardini analytical solution the domain is divided into three regions (Fig. 5): unfrozen, partially frozen (or mushy), and fully frozen. The domain is initially unfrozen with $T = T_0$. At the left boundary condition a Dirichlet boundary condition is imposed with $T(x = 0, t) = T_s$, and the right boundary temperature is kept equal to the initial condition, $T(z \to \infty, t) = T_0$.

https://doi.org/10.5194/tc-2020-293
Preprint. Discussion started: 19 October 2020

The Cryosphere Discussions
Open Access
EGU

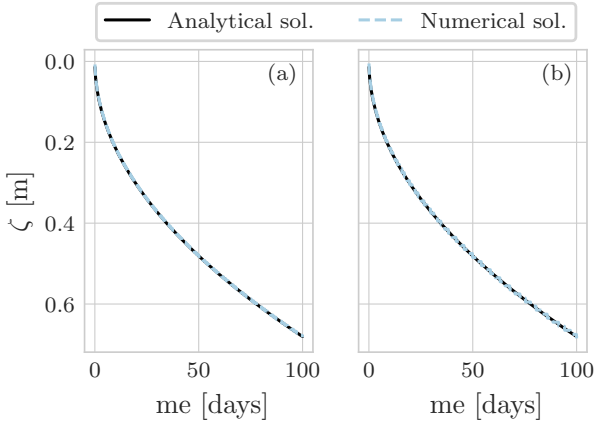

Figure 3. Propagation of the freezing front compared between the Neumann analytical and the numerical solution with the NCZ algorithm. Two space discretizations are used: (a) $\Delta z = 0.005$ m, and (b) $\Delta z = 0.01$ m. The integration time step is $\Delta t = 3600$ s.

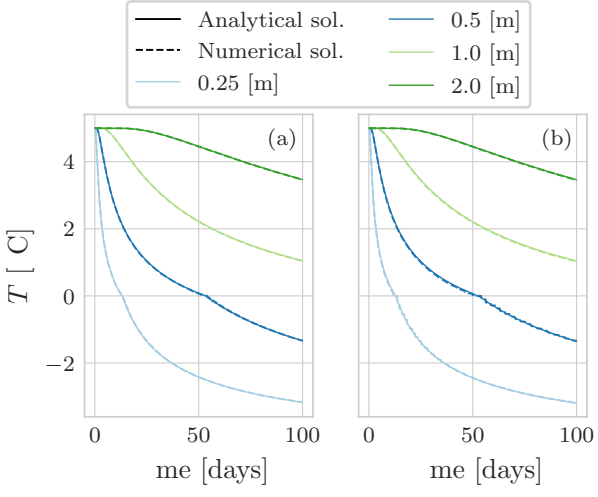

Figure 4. Temperature evolution for the Neumann analytical and the numerical solution with the NCZ algorithm at various depths. The space discretizations are used: (a) $\Delta z = 0.005$ m, and (b) $\Delta z = 0.01$ m. The integration time step is $\Delta t = 3600$ s.

We computed benchmark T1 proposed by the InterFrost project (InterFrost Project), parameters are given in Table (F1). The model agrees well with the analytical solution for all the three cases of T_m in terms of both the temperature profile, Fig. (6) and Tab. (3), and the freezing front position, Fig. (7) and Tab. (4), even with an hourly time step.

For comparison, McKenzie et al. (2007) compared the numerical model SUTRA against the Lunardini analytical solution for the cases $T_m = -4$ °C and $T_m = -1$ °C using a time step size of 900 s and a space resolution of 0.01 m. For the first test case the maximum absolute error was 0.01 °C, and for the second 0.1 °C. Their parameters, however, differ from those suggested by

https://doi.org/10.5194/tc-2020-293
Preprint. Discussion started: 19 October 2020

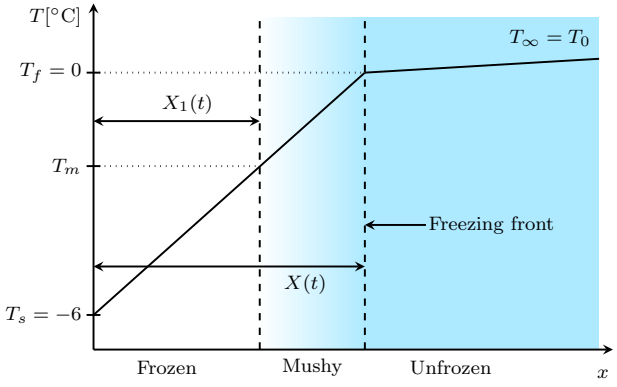

Figure 5. Scheme showing the setting of Lunardini problem (Ruhaak et al., 2015). Initially the domain is unfrozen with $T = T_0$. $X_1(t)$ and $X(t)$ identify respectively the isotherm corresponding to T_m and T_f, i.e. the mushy region.

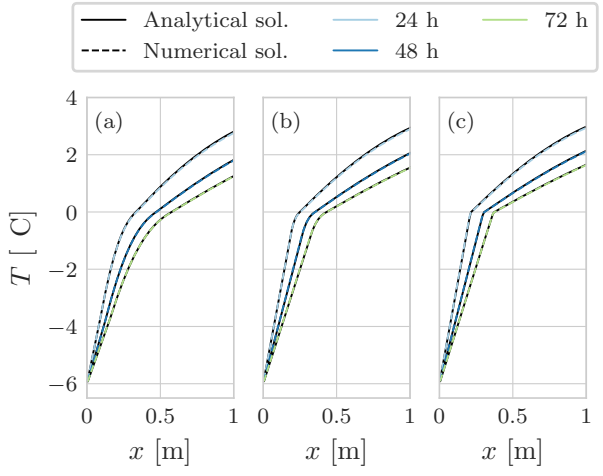

Figure 6. Comparison between the Lunardini solution and the numerical solution with the NCZ algorithm for the three cases of T1 benchmark: (a) $T_m = -4$ °C, (b) $T_m = -1$ °C, (c) $T_m = -0.1$ °C. The colours represent different times frame. The integration time step is $\Delta t = 3600$ s, and the space resolution is $\Delta x = 0.01$ m.

the InterFrost consortium, making performance comparisons difficult. In particular, their porosity was $0.05\ \mathrm{m^3 m^{-3}}$, whereas InterFrost uses $0.336\ \mathrm{m^3 m^{-3}}$. As this determines the amount of latent heat involved in phase change, smaller errors are to be suspected to occur with the parameters used by McKenzie et al. (2007).

https://doi.org/10.5194/tc-2020-293
Preprint. Discussion started: 19 October 2020

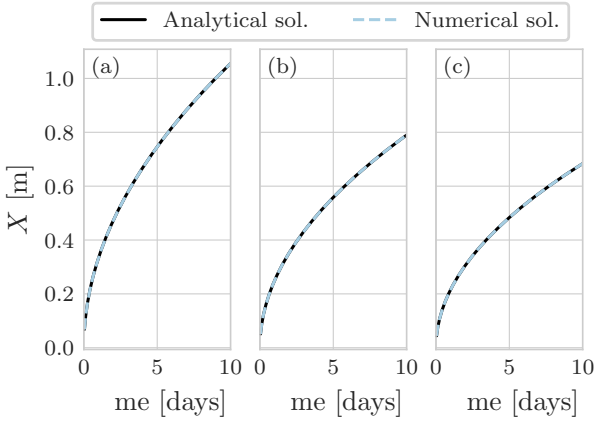

Figure 7. Propagation of the zero-isotherm for the Lunardini solution and the numerical solution with the NCZ algorithm for the three cases of T1 benchmark: (a) $T_m = -4$ °C, (b) $T_m = -1$ °C, (c) $T_m = -0.1$ °C. The integration time step is $\Delta t = 3600$ s, and the space resolution is $\Delta x = 0.01$ m.

Table 3. Maximum absolute error °C of the temperature after 24 h from the numerical solution with the NCZ algorithm relative to the Lunardini analytical solution. The space resolution is $\Delta x = 0.01$ m.

	$T_m = -4$ °C	$T_m = -1$ °C	$T_m = -0.1$ °C
$\Delta t = 300$ s	0.00683	0.01419	0.11436
$\Delta t = 900$ s	0.01496	0.02448	0.11565
$\Delta t = 3600$ s	0.05115	0.08286	0.12116

5 Numerical test

In the previous sections, we have demonstrated that the proposed method can reproduce the Neumann analytical solution, as well as the Lunardini analytical solution, even when using larger time steps than other numerical models.

After comparing simulation results with analytical solutions, we now analyse the difference between solutions using hourly, daily, and 10-day time steps. The domain is a soil column of 20 m depth that is uniformly at $T = -3$ °C, initially. The bottom boundary condition is adiabatic and at the surface, we use a Dirichlet boundary condition. The original forcing has hourly resolution and for longer time steps, corresponding averages are computed. As temperature gradients and the influence of phase change are usually greatest near the soil surface, the thickness Δx is parameterized with an exponential function (Gubler et al., 2013)

$$\Delta x_i = \Delta x_{min}(1+b)^{i-1} \tag{24}$$

https://doi.org/10.5194/tc-2020-293
Preprint. Discussion started: 19 October 2020


The Cryosphere Discussions
Open Access
EGU

Table 4. Maximum error m of the freezing front position from the numerical solution with the NCZ algorithm relative to the Lunardini analytical solution. The space resolution is $\Delta x = 0.01$ m.

	$T_m = -4$ °C	$T_m = -1$ °C	$T_m = -0.1$ °C
$\Delta t = 300$ s	0.00032	0.00051	0.00001
$\Delta t = 900$ s	0.00043	0.00027	0.00016
$\Delta t = 3600$ s	0.00062	0.00057	0.00047

where Δx_{min} is the thickness of the first layer, b is the growth rate and i is the layer index, being one at the ground surface and increasing downward. The parameters used are reported in Table H1. All three simulations were spun-up for a period of 1400 years to reach a stable thermal regime. After spin-up, we performed a simulation of 100 years.

Figure (8) compares the zero-isotherm position computed after 100 years for the three different time steps. Interestingly, there are no significant deviations in the results. The larger deviations occur when the zero-isotherm is shallow: at the beginning of the thawing season as well as the freezing one, Fig. (H1, H2). This can be attributed on one side to the diurnal cycles of surface boundary condition, and on the other side that using a larger time step we lose accuracy in capturing the timing of thawing/freezing even if we use the same boundary condition.

With larger time steps, we lose some of the information of the boundary conditions and the accuracy of the numerical model decreases because it is first-order accurate in time. The overall performance relative to simulations with smaller time steps, however, is largely preserved. While the order of accuracy can be increased to second order in time using the Crank-Nicholson method, this would incur a time step restriction to guarantee the monotonicity of the solution. As this restriction is proportional to the square of the space discretization, Δx^2, the Crank-Nicholson method would represent a severe constrain whenever high spatial resolution is required.

Figure (9) compares the minimum, mean, and maximum temperature profile respectively for the three simulations. (a) shows the ground temperature envelope for the hourly simulation. The maximum envelop presents an 'elbow' that is due to the phase-change effects Fig. (H3). As can be seen in (b) and (d), close to the soil surface the hourly simulation presents larger values for both the minimum and maximum temperature due the fact that the hourly boundary condition presents a greater amplitude that is smoothed computing the daily and 10-day average.

In the mean temperature profile, the 10-day simulation presents a larger deviation from the hourly simulation than the daily simulation. The large deviation can be explained with the interaction of the time-step size with the thermal offset effect (Fig. H4). If the thermal conductivity of water is set equal to that of ice, the maximum difference between the three profiles is reduced to 0.003 °C with a maximum deviation of 0.003 °C from the initial condition, that is also equal to the mean of the forcing boundary condition.

Regarding the spatial discretization Fig. (H5) reports a comparison of the zero-isotherm position obtained using an hourly time step, a daily time step, and a 10 day time step. The results are still in good agreement, but is it interesting to note that the zero-isotherm presents some steps, independently on the size of the time step, and some details are missed, such as the joining

https://doi.org/10.5194/tc-2020-293
Preprint. Discussion started: 19 October 2020

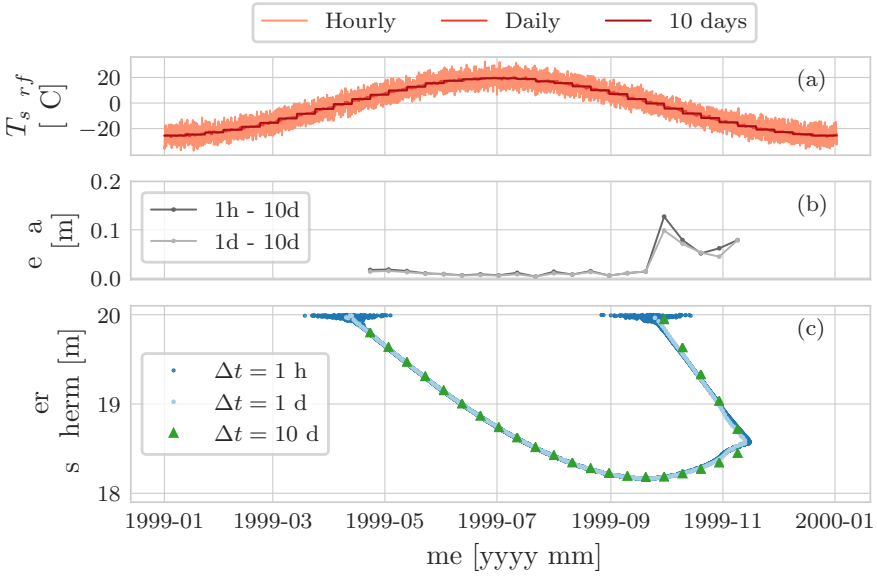

Figure 8. Comparison of the position of the zero-isotherm after 100 years of three simulations: using an hourly boundary condition with time step of $\Delta t = 1$ h, using a daily boundary condition with a time step of $\Delta t = 1$ day, and a 10-day boundary condition with a time step of $\Delta t = 10$ day.

of the downward and upward freezing fronts captured with the finer grid. These steps are caused by the greater thickness of the grid elements. Because temperature is computed in the middle of each control volume, more time is required to achieve complete phase change of water, resulting in slower variation of the zero-isotherm position.

These synthetic experiments demonstrate that spatial and temporal discretization can be chosen to match the the aim of a study without constrains due to the convergence and stability issues of the numerical scheme.

6 Conclusions

We have presented a new model for simulating the ground thermal regime in the presence of freezing and thawing based on the heat-transfer equation and the application of the NCZ algorithm. To our knowledge, this is the only method that guarantees convergence while also permitting large time steps. The numerical model was implemented and verified against the Neumann and Lunardini analytical solutions. In both cases, the results were in good agreement even with an hourly integration time step. For the Neumann solution, we considered pure water instead of saturated soil since it is more numerically demanding, and no convergence problems were encountered despite choosing a narrow temperature range (0.0001 °C) over which phase change occurs.

Numerical experiments demonstrated the robustness of the model by comparing results at differing temporal and spatial resolutions. Results obtained with time steps of 1 h, 1 day, and 10 days are consistent. The robustness of the numerics allows

https://doi.org/10.5194/tc-2020-293
Preprint. Discussion started: 19 October 2020

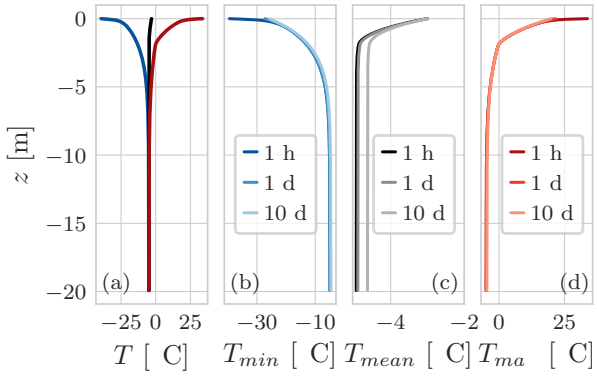

Figure 9. (a) The minimum, mean, and maximum temperature profile for the hourly simulation. (b), (c), (d) show the comparison of the minimum, mean, and maximum temperature profile respectively for the three simulations: with an hourly air temperature boundary condition and $\Delta t = 1$ h, with a daily air temperature boundary condition and $\Delta t = 1$ day, with a ten day air temperature boundary condition and $\Delta t = 10$ day. All three simulations last 100 years. The maximum difference of T_{mean} between the hourly, and daily simulation is of 0.04 °C, while between the hourly, and ten-days simulation is of 0.3 °C.

the user to choose both the space and time discretization without any restriction due to stability and convergence issues. As a consequence, this method is effective for simulating permafrost thaw, a phenomenon that occurs at depth, in response to seasonal and multi-annual cycles, and often over tens, hundreds or even thousands of years. Furthermore, phenomena like hysteresis or the variation of solute concentration upon freezing (Clow, 2018) can be included in the numerical model if the enthalpy function (i.e. its parameters) does not change within the current time step of integration.

While we presented a finite volume method, the NCZ algorithm can be also for finite differences and finite elements methods. Beyond applications to frozen soil, it can be used to study other geophysical phenomena that involve phase change of a substance simply by changing the definition of the enthalpy function and the thermal conductivity function. Examples include, glacier dynamics (Aschwanden et al., 2012), snow pack evolution (Brun et al., 1992; Lehning et al., 1999), and magma bodies (De Lorenzo et al., 2006). This may be even further expanded to industrial problems involving phase change materials used in energy recovery systems (Mongibello et al., 2018; Nazzi Ehms et al., 2019) or casting problems of pure metals and alloys (Lewis and Ravindran, 2000).

Code availability. The model theory is developed for the general three-dimensional case, the software developed, at present, performs one dimensional integration. The source code is written in Java using the object-oriented programming paradigm. The solver, FreeThaw1D, is deployed as an open source code to work alone or inside the Object Modelling System version 3 framework (David et al., 2013). In the latter case it can be connected at run time with the many other components developed along with the GEOframe system (Formetta et al., 2014; Bancheri, 2017) for providing hydrometeorological forcings and other fluxes, like the evapotranspiration. The source code can be found at https:

https://doi.org/10.5194/tc-2020-293
Preprint. Discussion started: 19 October 2020

//github.com/geoframecomponents/FreeThaw1D (Tubini, c). The OMS3 project can be found at https://github.com/GEOframeOMSProjects/OMS_FreeThaw1D (Tubini, b). The results presented here can be found at http://dx.doi.org/10.5281/zenodo.4017668 (Tubini, a).

Appendix A: Commonly used simulation software

The heat equation can be written in different forms that are analytically equivalent, but subject to differing numerical advantages and disadvantages. In the scientific literature, several simulators, i.e. software that implements a particular model (set of equations), for solving the heat equation with freezing and thawing have been presented. Here we review commonly used frozen soil models in terms of their governing equations and methods of finding numerical solutions.

Heat transfer with phase change of water is a cross-cutting problem existing in many geophysical phenomena other than frozen soil. This includes, for example, the seasonal snow pack, glaciers, and ice-sheets. Our contribution does not seek to present an improvement in the description of these problems and we ignore typical processes such as metamorphism and settling in seasonal snow or strain heating and deformation in glaciers and ice sheets. Nevertheless, corresponding models may benefit from the NCZ algorithm in the treatment of the nonlinearity arising from phase change and, furthermore, broadening our review to also include some snow and glacier models supports the generalisation of our findings.

A1 CLM

The Community Land Model (CLM) is the LSM for the Community Earth System Model (Oleson et al., 2004). It includes a module to simulate the ground temperature considering freezing and thawing. The governing equation is written in the non-conservative form and does not include the latent heat term (Oleson et al., 2004) (Lawrence et al., 2019). The heat conduction equation is solved using a Crank-Nicholson method. The temperature profile is calculated adopting the DECP approach. This approach does not require to solve a nonlinear system, since the latent heat is treated in an explicit way, but Nicolsky et al. (2007a) have pointed out that this two-step procedure can overestimate the region where the phase change occurs, resulting in inaccuracies in the simulation of active-layer thickness.

A2 CoupModel

The CoupModel (Jansson and Karlberg, 2011) is a one-dimensional numerical model to simulate the heat and water flow as well as carbon and nitrogen budgets in a soil-plant-atmosphere system (Hollesen et al., 2011). The governing equation for heat flow in the soil is defined using the apparent heat capacity, and solved with an explicit numerical method. This does not require to solve a non-linear system but sets a time step restriction to avoid numerical oscillation.

A3 CryoGrid

CryoGrid 2 simulates the ground thermal regime based on conductive heat transfer in the soil and in the snowpack (Westermann et al., 2013). The heat equation is written using the apparent heat capacity and solved using the method of lines (Westermann et al., 2013). The resulting system of ordinary differential equations is solved numerically with the package CVODE of Sundials

https://doi.org/10.5194/tc-2020-293
Preprint. Discussion started: 19 October 2020

that implements a modified Newton method, and Inexact Newton method, or a fixed-point solver to linearize the algebraic system resulting from the discretization of the heat transfer equation. To our knowledge there is no mathematical proof that these algorithm converge to the exact solution.

A4 GEOtop

GEOtop (Rigon et al., 2006; Endrizzi et al., 2014) is a physically based distributed model of the mass and energy balance of the hydrological cycle. It includes a module for solving the energy equation in freezing soil (Dall'Amico et al., 2011); this module can also be linked with the solver for the Richards equation. The governing equation for heat transfer is written in conservative form, but when solving the equation the apparent heat capacity formulation is used. A globally convergent Newton algorithm is used to deal with the non-linearities arising from phase change (Dall'Amico et al., 2011). The globally convergent Newton represents an improvement over the Newton-Rapshon algorithm but it does not guarantee convergence of the solution, and as presented in Appendix (G), the choice of the parameter δ is non trivial.

A5 GIPL-2.0

GIPL-2.0 simulates the ground thermal regime by solving the heat equation with phase change numerically (Marchenko et al., 2008). The governing equation is written in the conservative form and Newton's method is used to linearize the energy equation. To overcome convergence problems when solving the non-linear system, GIPL-2.0 implements a fractional time step approach, Godunov splitting. The key point of the solution regards the treatment of the enthalpy time derivative: in case of a non zero gradient of temperature exists the time derivative is approximated with a difference derivative, otherwise using the analytical representation.

A6 Goodrich

Goodrich (1982) presented a one-dimensional model to simulate the ground thermal regime considering the phase change of water. The governing equation is written in the non conservative form and does not include the latent heat of fusion. Phase change is treated with the front tracking method, which offers good accuracy for problems in which phase change occurs at a fixed temperature (Goodrich, 1982). This model does not use a SFCC, and instead, the soil is represented as homogeneous layers with distinct frozen and thawed thermal properties.

A7 Hydrus 1D

Hydrus 1D includes a module to simulate water flow and heat transport in frozen soil. The governing equation is written using the apparent heat capacity formulation and Picard iteration is used to linearize the algebraic nonlinear system. In their paper, Hansson et al. (2004) explain that during the Picard iteration the solution can easily oscillate whenever the temperature decrease below the melting temperature. To avoid these oscillation the temperature is reset to the critical value and iteration restarted. Hydrus 1D adopts an empirical time-step adaptation criterion. It is worthwhile to notice that the modified Picard iteration was

https://doi.org/10.5194/tc-2020-293
Preprint. Discussion started: 19 October 2020

proposed by Celia et al. (1990) to solve the Richards equation – problem for which the NCZ algorithm was originally proposed (Casulli and Zanolli, 2010).

A8 MarsFlo

MarsFlo is a three-phase numerical model to simulate the heat transfer and water flow in partially frozen, partially saturated porous media (Painter, 2011). The heat equation is written in the conservative form. The equation is solved using an implicit finite difference method, and the resulting nonlinear system is solved using a Newton-Raphson method. To overcome convergence and stability problems, three modification were introduced (Painter, 2011). There is no mathematical proof that this modified Newton-Raphson algorithm converges.

A9 NEST

Zhang et al. (2003) developed a one-dimensional physically based model of Northern Ecosystem Soil Temperature (NEST). The heat equation is written in the source term formulation and solved with the DECP approach. The numerical method is explicit in time, thus the maximum time step is of 30 minutes to prevent oscillations in the solution.

A10 Sergueev et al.

This is a two dimensional model and the governing equation is written in the enthaply form (Sergueev et al., 2003). This model implements a fractional time step approach (Godunov splitting): each time step is divided into two steps and at each step, a different dimension is treated implicitly. The system of finite difference equations is non-linear and is solved with the Newton's method. As in GIPL-2.0, the time derivative of enthalpy is computed either using the difference derivative or the analytical derivative according with the gradient of the temperature field.

A11 SoilVision

The heat equation is written using the apparent heat capacity. The equation are solved using a finite element solver, FlexPDE suite, both explicit and implicit in time. In case of implicit methods, the resulting non-linear system is solved using the Newton-Raphson method. In the presence of nonmonotic functions, the Newton-Raphson method may fail to converge to the exact solution.

A12 SUTRA

SUTRA is an established USGS groundwater flow and coupled transport model (Voss and Provost, 2002). McKenzie et al. (2007) and McKenzie and Voss (2013) have extended the model to simulate freezing and thawing processes in the soil. The heat equation is written using the apparent heat capacity formulation and nonlinearities are solved using Picard iteration. Picard iteration does not guarantee to converge to the exact solution.

https://doi.org/10.5194/tc-2020-293
Preprint. Discussion started: 19 October 2020

A13 Crocus

Crocus is a one-dimensional finite difference model that solves the mass and energy balance within the snowpack taking into account metamorphism and settling. The first versions of Crocus (Brun et al., 1989, 1992) were not enthalpy-based. The governing equation was written in terms of temperature and water content. It is solved by using the Crank-Nicholson method, and the phase change is treated by using the DECP approach (Brun et al., 1992). After the integration within SURFEX (Vionnet et al., 2012), Crocus uses the enthalpy formulation and the numerical scheme is fully implicit, based on the numerics of ISBA-ES (Boone and Etchevers, 2001). Similarly to the previous version, the heat balance equation is solved adopting the DECP approach (Boone and Etchevers, 2001). D'Amboise et al. (2017) implemented a routine for water flow in the snowpack based on the Richards equation, which is characterized by nonlinear behaviour like the enthalpy equation. To solve it, they adopted an approach based on Picard iteration with variable time steps (Paniconi and Putti, 1994).

A14 SNOWPACK

SNOWPACK (Lehning et al., 1999) solves the heat transfer and creep/settlement equations using a Lagrangian finite element method. The governing equation is written using the source/sink formulation and the phase change between ice and water components are accounted for as volumetric heat sinks (melting) and sources (refreezing) (Bartelt and Lehning, 2002; Lehning et al., 1999). Regarding the water flow, SNOWPACK implements three different schemes: a simple bucket-type approach, an approximation of Richards equation, and the full Richards equation cite(Wever). The full Richards equation is solved using Picard iteration with variable time steps (Paniconi and Putti, 1994).

A15 Ice-sheet models

For glacier and ice-sheet models it is necessary to distinguish between cold and temperate ice. Following Aschwanden and Blatter (2005), "ice is treated as temperate if a change in heat content leads to a change in liquid water content alone, and is considered cold if a change in heat content leads to a temperature change alone." This means that cold ice is always below the melting temperature and thus the phase change does not occur. As result, present-day ice sheet models can be classified into: 'cold-ice method' models and polythermal models.

'Cold-ice method' does not consider the phase change of ice. Because of this the heat capacity can be assumed to be constant and therefore the governing equation can be written in terms of only temperature. These models are easy to implement, but their applicability is restricted since in general temperate zones can be present (Aschwanden and Blatter, 2009). In fact, since the phase change of ice is overlooked, locally, the 'cold-ice method' violates the energy conservation, overestimates the temperate region (Aschwanden and Blatter, 2009), and can not quantify the liquid water content that affects viscosity in temperate ice (Lliboutry and Duval, 1985).

By contrast, polythermal ice-sheet models consider the phase change of ice. Similar to freezing soil models, the polythermal ice-sheet models can be classified in two groups on the base of the treatment of the phase change: front tracking method and enthalpy method (Nedjar, 2002). SICOPLOIS (Greve, 1997a, b; Greve and Blatter, 2016) is the only 'truly' polythermal

https://doi.org/10.5194/tc-2020-293
Preprint. Discussion started: 19 October 2020

ice sheet model. It employs the polythermal two-layer scheme (Greve, 1997b): the temperature field and the water content field are computed separately for the ice and temperate domain and a Stefan-type condition is applied at the cold-temperate surface (CTS). This model defines the CTS for both energy flux and mass flux. The drawback of this method relate to the implementation and restriction on the geometry and topology of the CTS (Aschwanden et al., 2012).

Aschwanden and Blatter (2009) presented an enthalpy gradient method. This is a fixed-grid method that differs from the enthalpy method commonly used for freezing soil in its definition of the energy flux. In the enthalpy method, the heat flux is expressed in terms of the temperature gradient, whereas in the enthalpy gradient method it is expressed in terms of enthalpy, assuming that the heat capacity is constant (Aschwanden and Blatter, 2009). The enthalpy approach combines the advantage of solving one equation for the entire domain, cold-ice models, and the correct description of the thermodynamics of temperate ice (front tracking model). This model is implemented in COMSOL Multiphysics (Aschwanden and Blatter, 2009), where nonlinear problems are solved using either a Newton algorithm or a damped Newton algorithm. Also in this case the NCZ may represent a valid option to solve the nonlinear system. To the authors' knowledge, the enthalpy gradient method has not be used in freezing soil models.

Appendix B: Pseudocode

We present the pseudocode for a one-dimensional implementation of the NCZ algorithm. Since the matrix $\mathbf{A}$ in Eq. (16) is tri-diagonal we can efficiently compute only the non-zero diagonal: the upper diagonal, the main diagonal, and the lower diagonal. We use the generic expression *Discretize the governing equation* since here, we can choose to adopt either a finite volume method, as presented in this paper, a finite element method, or a finite difference method. Moreover, the matrix $\mathbf{A}$ is symmetric and positive definite thus within the nested Newton algorithm the linearized algebraic system can be easily solved with the Thomas algorithm. Here, it is worthwhile to point out that when we move to the two-dimensional or three-dimensional problem, the linearized algebraic system cannot be solved with the Thomas algorithm as the matrix is no longer tri-diagonal. In these cases, iterative schemes such as the Conjugate Gradient Method need to be used (Shewchuk, 1994).

Appendix C: Enthalpy and internal energy

Following the work by Dall'Amico (2010), the internal energy in its canonical form, U_c, can be written as

$$U_c = U_c(S, V, M) \tag{C1}$$

where S is the entropy, V is the volume, and M the mass of the constituents. These are the independent variables and are called extensive variables since they depend linearly on the mass of the substance. The first differential of Eq. (C1) is

$$dU_c = \left(\frac{\partial U_c}{\partial S}\right) dS + \left(\frac{\partial U_c}{\partial V}\right) dV + \left(\frac{\partial U_c}{\partial M}\right) dM \tag{C2}$$

According to Callen (1985) it is possible to define

$$\left(\frac{\partial U_c}{\partial S}\right) \equiv T\text{, the temperature} \tag{C3}$$

https://doi.org/10.5194/tc-2020-293
Preprint. Discussion started: 19 October 2020

The Cryosphere Discussions
Open Access
EGU

Algorithm 1 Program flow

Read inputs
for $time = 1, 2, \ldots$ **do**
  read boundary conditions
  compute enthalpy and thermal conductivity at time level $time$
  Discretize the governing equation
  for $i = 1, 2, \ldots, N_v$ **do**
    Compute the matrix entries and rhs of the system applying the boundary condition when $i == 1$ and $i == N_v$
  end for
  Solve the non-linear system: nested Newton algorithm
  Choose the initial guess
  $T_i^0 = \min(T_i^n, T^*)$
  for $k = 1, 2, \ldots$, outer iteration **do**
    linearize h_2
    for $m = 1, 2, \ldots$, inner iteration **do**
      linearize h_1
      for $i = 1, 2, \ldots, N_v$ **do**
        compute
        $d_k = -H_1(T_k^{i,m-1}) + (H_2(T_k^i) - Q(T_k^i)(T_k^{i,m-1} - T_k^i)) + rhs_k$
      end for
      solve the linear system with the Thomas algorithm
      $(\mathbf{A} + \boldsymbol{P}^{k,m-1} - \boldsymbol{Q}^{k-1})\boldsymbol{T}^{k,m} = \boldsymbol{D}$
      compute the residual of the inner iteration
      $innerRes = \boldsymbol{P}^{k,m-1}(\boldsymbol{T}^{k,m-1} - \boldsymbol{T}^{k,m}) - (\boldsymbol{H_1}^{k,m-1} - \boldsymbol{H_1}^{k,m})$
      if $innerRes < tolerance$ **then**
        $\boldsymbol{T}^k = \boldsymbol{T}^{k,m}$
      end if
    end for
    compute the residual of the outer iteration
    $outerRes = \boldsymbol{H}^{k-1}(\boldsymbol{T}^{k-1} - \boldsymbol{T}^k) - (\boldsymbol{H_2}^{k-1} - \boldsymbol{H_1}^k)$
    if $outerRes < tolerance$ **then**
      $\boldsymbol{T} = \boldsymbol{T}^k$
    end if
  end for
end for

https://doi.org/10.5194/tc-2020-293
Preprint. Discussion started: 19 October 2020

$$-\left(\frac{\partial U_c}{\partial V}\right) \equiv p\text{, the pressure} \tag{C4}$$

$$\left(\frac{\partial U_c}{\partial M}\right) \equiv \mu\text{, the chemical potential} \tag{C5}$$

With this notation, Eq. (C2) becomes

$$dU_c = TdS - pdV + \mu dM \tag{C6}$$

By making use of the Legendre transformation it is possible to define the enthalpy potential H_c as

$$H_c(S,p,M) = U_c(S,V,M) + pV(S,p,M) \tag{C7}$$

The differential of the enthalpy is

$$dH_c = d[U_c + pV] = TdS - pdV + \mu dM + Vdp + pdV =$$
$$TdS + \mu dM + Vdp \tag{C8}$$

If we assume that the transformation occurs at constant pressure and volume then Eq. (C6) becomes

$$dU_c = TdS + \mu dM \tag{C9}$$

and Eq. (C8)

$$dH_c = TdS + \mu dM \tag{C10}$$

Hence, from Eq. (C9) and Eq. (C10) the differential of the internal energy and the differential of enthalpy are equal. Therefore the governing equation, Eq. (1), can be equivalently written in term of either the specific enthalpy or the specific internal energy.

Appendix D: Neumann analytical derivation

In this section we report the derivation of the Neumann analytical. The enthalpy is defined as

$$h(T) = \begin{cases} \rho_w c_w (T - T_{ref}) + \rho_w l_f & \text{if } T \geq T_m \\ \rho_i c_i (T - T_{ref}) & \text{if } T < T_m - \epsilon \\ \rho_i c_i (T - \epsilon - T_{ref}) + h^{'}(T - (T_m - \epsilon)) & \text{otherwise} \end{cases} \tag{D1}$$

where the singularity of the enthalpy function at $T = T_m$ has been linearized with

$$h^{'} = \frac{\rho_w c_w (T_m - T_{ref}) + \rho_w l_f - \rho_i c_i (T_m - \epsilon - T_{ref})}{\epsilon} \tag{D2}$$

https://doi.org/10.5194/tc-2020-293
Preprint. Discussion started: 19 October 2020

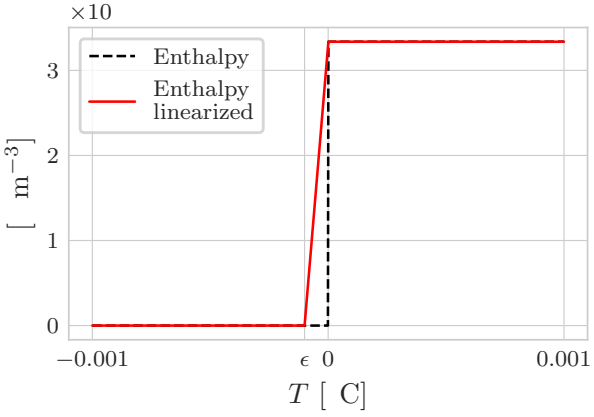

Figure D1. Comparison between the enthalpy fucntion of pure water and the enthalpy function used in the numerical model. Note that the energy jump due to the latent heat at $T_m = 0$ °C has been linearized and the steepness is controlled by the parameter ϵ.

and ϵ is a parameter defining the temperature range over which the phase change of water occurs, Fig. (D1). In the following tests ϵ is set to be equal to 0.0001 °C. Even though the internal energy function is very steep, the code used does not suffer of convergence problem with a time step of 3600 s. The thermal conductivity is defined as:

$$\lambda(T) = \begin{cases} \lambda_w & \text{if } T \geq T_m \\ \lambda_i & \text{if } T < T_m \end{cases} \tag{D3}$$

Defining the following constant:

$$\alpha_w = \frac{\lambda_w}{\rho_w c_w} \quad \alpha_i = \frac{\lambda_i}{\rho_i c_i} \tag{D4}$$

$$A = \frac{T_m - T_s}{\text{erf}(\gamma)} \quad B = \frac{T_m - T_0}{\text{erf}\left(\gamma\sqrt{\frac{\alpha_i}{\alpha_w}}\right)} \tag{D5}$$

the moving boundary function is

$$\zeta(t) = 2\gamma\sqrt{\alpha_i t} \quad \textit{for } t > 0 \tag{D6}$$

where the coefficient γ can be found solving the following equation

$$\gamma\sqrt{\alpha_i} l_f \rho - \frac{\lambda_i}{\sqrt{\pi\alpha_i}} A e^{-\gamma^2} - \frac{\alpha_w}{\sqrt{\pi\alpha_w}} B e^{\gamma^2 \frac{\alpha_i}{\alpha_w}} = 0 \tag{D7}$$

https://doi.org/10.5194/tc-2020-293
Preprint. Discussion started: 19 October 2020


The Cryosphere Discussions

Table D1. Input parameters for the comparison between Neumann analytical solution and the numerical solution.

Symbol	Parameter	Value	Unit
Δt	time step	60, 300, 3600	s
Δz	control volume size	0.001, 0.005, 0.01	m
l_f	latent heat of fusion	333700	J kg^{-1}
c_w	specific heat capacity of water	4187	J m^{-3} °C^{-1}
c_i	specific heat capacity of ice	2108	J m^{-3} °C^{-1}
ρ_w	water density	1000	kg m^{-3}
ρ_i	ice density	970	kg m^{-3}
λ_w	thermal conductivity of water	0.6	W m^{-1} °C^{-1}
λ_i	thermal conductivity of ice	2.09	W m^{-1} °C^{-1}
ϵ	melting temperature range	0.0001	°C
T_0	initial temperature	$-5, +5$ [a]	°C
T_s	surface temperature	$+5, -5$ [a]	°C

[a] We tested the code both for the freezing case and the thawing case. The thawing case is reported in the Appendix. The first value refers to the freezing case and the second one to the thawing case.

Finally the analytical solution for problem with Dirichlet boundary condition for the thawed and frozen zones are:

$$\begin{cases} T(z,t) = T_s + \dfrac{T_m - T_s}{\mathrm{erf}(\gamma)} \mathrm{erf}\left(\dfrac{z}{2\sqrt{\alpha_i t}}\right) & 0 < z < \zeta(t) \\ T(z,t) = T_0 + \dfrac{T_m - T_0}{\mathrm{erfc}\left(\gamma\sqrt{\dfrac{\alpha_i}{\alpha_w}}\right)} \mathrm{erfc}\left(\dfrac{z}{2\sqrt{\alpha_w t}}\right) & z > \zeta(t) \end{cases} \tag{D8}$$

Appendix E: Neumann solution for melting ice

Kurylyk et al. (Kurylyk et al., 2014b) recommended to include as benchmark the Neumann solution with initial temperature less than 0 °C.

Appendix F: Lunardini analytical derivation

The Lunardini solution as described by McKenzie (McKenzie et al., 2007) is given by the following set of equations:

$$T_1 = (T_m - T_s)\frac{\mathrm{erf}\left(\dfrac{x}{2\sqrt{\alpha_1 t}}\right)}{\mathrm{erf}(\psi)} + T_s \tag{F1}$$

https://doi.org/10.5194/tc-2020-293
Preprint. Discussion started: 19 October 2020

The Cryosphere
Discussions
Open Access
EGU

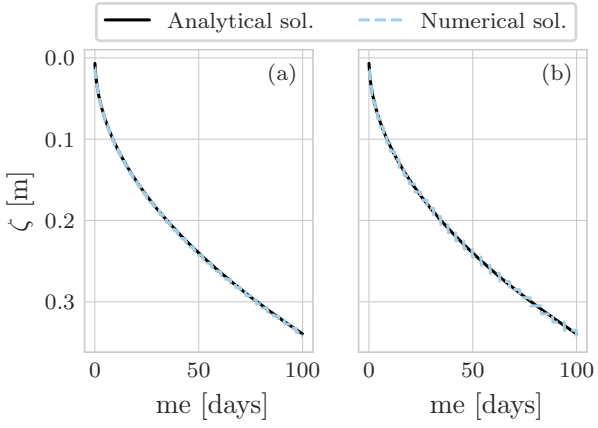

Figure E1. Comparison between the Neumann analytical solution and the numerical solution with the nested Newton algorithm for two different space discretization: (a) $\Delta z = 0.005$ m (b) $\Delta z = 0.01$ m. The integration time step is $\Delta t = 3600$ s.

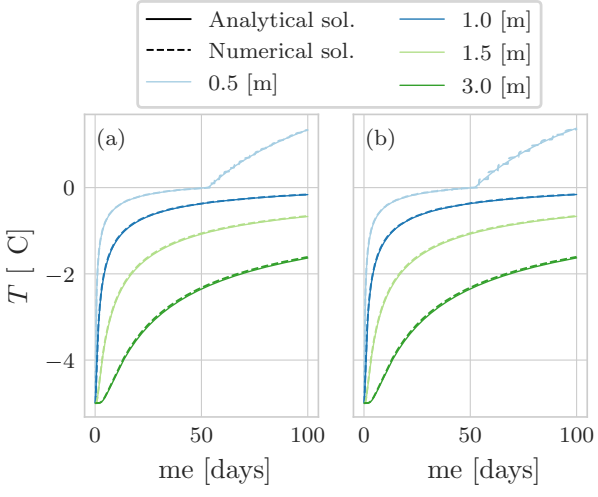

Figure E2. Propagation of the thawing front for the Neumann solution and the numerical solution with the nested Newton algorithm for two different space discretization: (a) $\Delta z = 0.005$ m, (b) $\Delta z = 0.01$ m. The integration time step is $\Delta t = 3600$ s.

535

$$T_2 = (T_m - T_f)\frac{\mathrm{erf}\left(\frac{x}{2\sqrt{\alpha_4 t}}\right) - \mathrm{erf}(\gamma)}{\mathrm{erf}(\gamma) - \mathrm{erf}\left(\psi\sqrt{\frac{\alpha_1}{\alpha_4}}\right)} + T_f \tag{F2}$$

https://doi.org/10.5194/tc-2020-293
Preprint. Discussion started: 19 October 2020


The Cryosphere Discussions
Open Access
EGU

Table E1. Maximum error m of the thawing front position for different space and time discretizations.

	$\Delta t = 60$ s	$\Delta t = 300$ s	$\Delta t = 3600$ s
$\Delta z = 0.001$ m	0.00084	0.00135	0.00614
$\Delta z = 0.005$ m	0.00432	0.00437	0.00546
$\Delta z = 0.01$ m	0.00853	0.00863	0.00927

$$T_3 = (T_0 - T_f)\frac{-\operatorname{erfc}\left(\frac{x}{2\sqrt{\alpha_3 t}}\right)}{\operatorname{erfc}\left(\psi\sqrt{\frac{\alpha_4}{\alpha_3}}\right)} + T_0 \tag{F3}$$

where T_1, T_2, and T_3 are the temperatures at distance, x, from the temperature boundary for the frozen, mushy, and unfrozen zone respectively; erf and $erfc$ are the error function, and the complementary error function respectively; T_0, T_m, T_f, and T_s are the temperatures of the initial condition; the solidus, the liquidus, and the boundary temperature, respectively; α_1 and α_3 are the thermal diffusivities for the frozen, and unfrozen zone respectively, defined as λ_1/C_1 and λ_3/C_3 where C_1 and C_3 are the volumetric bulk-heat capacities of the frozen and unfrozen zones. The thermal diffusivity of the mushy zone is assumed to be constant across the transition region, and the thermal diffusivity with latent heat term included, α_4, is defined as:

$$\alpha_4 = \frac{\lambda_2}{C_2 + \frac{\gamma_d l_f \Delta\xi}{(T_f - T_m)}} \tag{F4}$$

where γ_d is the dry unit of soil solids, and $\Delta\xi = \xi_0 - \xi_f$ where ξ_0 and ξ_f are the ratio of unfrozen water to soil solids for the fully thawed and frozen conditions respectively. For a time, t, in the region $0 \leq x \leq X_1(t)$ the temperature is T_1 and $X_1(t)$ is given by

$$X_1(t) = 2\psi\sqrt{\alpha_1 t} \tag{F5}$$

and from $X_1(t) \leq x \leq X(t)$ the temperature is T_2, where $X(t)$ is given by

$$X(t) = 2\gamma\sqrt{\alpha_4 t} \tag{F6}$$

and for $x \geq X(t)$ the temperature is T_3. The unknowns, ψ and γ, are solving the set of these two equations:

$$\frac{T_m - T_s}{T_m - T_f}\exp^{-\psi^2(1-\alpha_1/\alpha_4)} = \frac{\frac{\lambda_2}{\lambda_1}\sqrt{\frac{\alpha_1}{\alpha_4}}\operatorname{erf}(\psi)}{\operatorname{erf}(\gamma) - \operatorname{erf}\left(\psi\sqrt{\frac{\alpha_1}{\alpha_4}}\right)} \tag{F7}$$

$$\frac{(T_m - T_f)\frac{\lambda_2}{\lambda_3}}{T_m - T_f}\frac{\alpha_3}{\alpha_4}\exp^{-\gamma^2(1-\alpha_4/\alpha_3)} = \frac{\operatorname{erf}(\gamma) - \operatorname{erf}\left(\sqrt{\frac{\alpha_1}{\alpha_4}}\psi\right)}{\operatorname{erf}\left(\gamma\sqrt{\frac{\alpha_4}{\alpha_3}}\right)} \tag{F8}$$

https://doi.org/10.5194/tc-2020-293
Preprint. Discussion started: 19 October 2020

The Cryosphere Discussions
Open Access
EGU

Table F1. Input parameters for the comparison between Lunardini analytical solution and the numerical solution.

Symbol	Parameter	Value	Unit
Δt	time step	300, 900, 3600	s
Δz	control volume size	0.01	m
L_f	latent heat of fusion	334560	J kg^{-1}
C_1	volumetric heat capacity, frozen	690030	J m^{-3} °C^{-1}
C_2	volumetric heat capacity, mushy	690030	J m^{-3} °C^{-1}
C_3	volumetric heat capacity, unfrozen	690030	J m^{-3} °C^{-1}
γ_d	dry unit density of soil solids	1680	kg m^{-3}
ξ_0	ratio of liq. water to soil solids, unfrozen	0.2	-
ξ_f	ratio of liq. water to soil solids, frozen	0.0782	-
λ_1	thermal conductivity, frozen	3.462696	W m^{-1} °C^{-1}
λ_2	thermal conductivity, mushy	2.939946	W m^{-1} °C^{-1}
λ_3	thermal conductivity, unfrozen	2.417196	W m^{-1} °C^{-1}
γ	solution parameter for Eq. (F7) and Eq. (F8)	5.616, 2.060, 1.397 [a]	-
ψ	solution parameter for Eq. (F7) and Eq. (F8)	0.158, 0.137, 0.061 [a]	-
T_0	initial temperature	+4	°C
T_s	boundary temperature	−6	°C
T_f	liquidus temperature	0	°C
T_f	solidus temperature	−0.1, −1, −4	°C

[a] The first value refers to $T_m = -0.1$ °C the second value t$T_m = -1$ °C, and the third value to $T_m = -4$ °C.

Appendix G: Comparing the nested Newton algorithm with other approaches

As reported by Dall'Amico et al. (2011), Figure (G1) represents a well known case for which the Newton-Raphson algorithm can not converge. Instead, the solution continuously cycles between the values T^i and T^{i+1}. While the Newton-Raphson algorithm converges to the exact solution if a good initial guess for T^{i+1} exists, this represents a severe constraint for the reliable application of this iterative algorithm in a numerical model. An improvement of the Newton-Raphson algorithm can be obtained using the globally convergent Newton scheme (Dall'Amico et al., 2011). It uses the Newton-Raphson algorithm to provide the right search direction and, in order to avoid overshooting, a reduction factor δ is used to find the new estimate. This represents an improvement over the Newton-Raphson method, but its ability to converge depends on the choice of the parameter δ and on the treatment of the apparent heat capacity (Hansson et al., 2004; Nicolsky et al., 2007b; Dall'Amico et al., 2011). As such, this algorithm does not guarantees to converge for any time step size and the requirements for small time steps

https://doi.org/10.5194/tc-2020-293
Preprint. Discussion started: 19 October 2020

The Cryosphere Discussions
Open Access
EGU

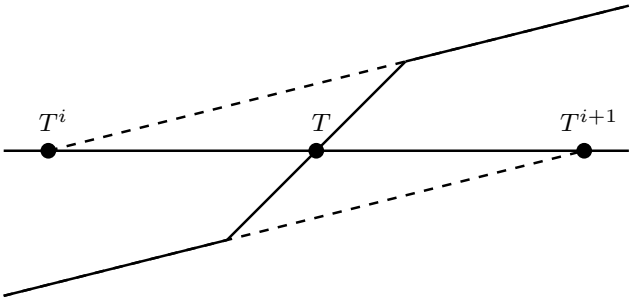

Figure G1. A scheme of problem which illustrates how the Newton-Raphson method can not converge towards T (Dall'Amico, 2010). In this case, the Newton-Raphson method fails to converge to T since it cycles between T^i and T^{i+1} values.

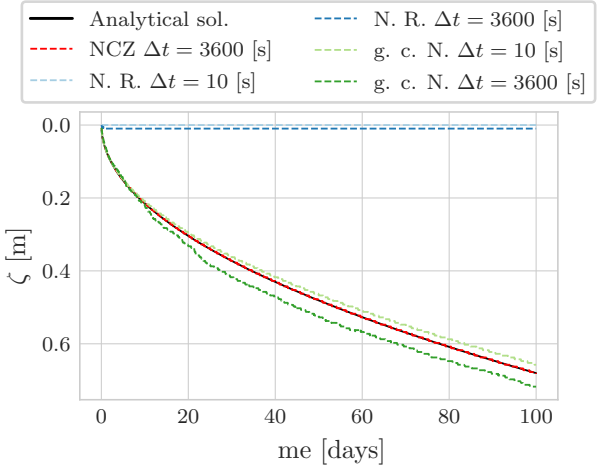

Figure G2. Comparison between the Neumann analytical solution and the numerical solution obtained with Newton-Raphson (N. R.), globally convergent Newton (g. c. N.), and NCZ algorithms. All the numerical simulations use the same spatial discretization $\Delta z = 0.005$ m.

can become a limiting factor. For example, in (Dall'Amico et al., 2011) the comparison between the Neumann solution and GEOtop has been done with a time step of 10 s.

A comparison of the numerical solutions obtained with the Newton-Raphson algorithm, globally convergent Newton algorithm, and the NCZ algorithm shows significant differences (Fig. G2). Newton-Raphson cannot reproduce the analytical solution even if a time step of $\Delta t = 10$ s is used. The globally convergent Newton is in good agreement with the analytical solution if $\Delta t = 10$ s. With an hourly time step, however, the example with the globally convergent Newton method is not able to reproduce the position of the freezing front over longer periods of time. By contrast, the NCZ algorithm reproduces the analytical solution well using $\Delta t = 3600$ s. The quality of the solution obtained with the globally convergent Newton algorithm depends not only on the time step duration but also on the definition of the parameter δ (Fig. G3). The additional

https://doi.org/10.5194/tc-2020-293
Preprint. Discussion started: 19 October 2020

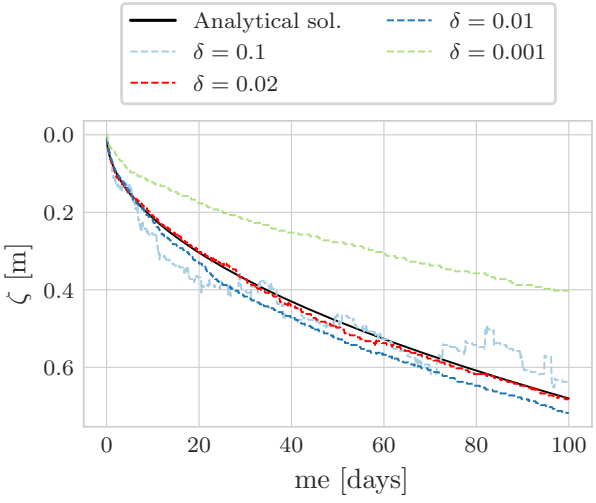

Figure G3. Comparison between the Neumann analytical solution and the numerical solution obtained with globally convergent Newton algorithm (g. c. N.). All the numerical simulations use the same spatial discretization $\Delta z = 0.005$ m and a time step size of $\Delta t = 3600$ s. This figure shows as the numerical solution depends on the choice of the parameter δ.

necessity for an arbitrarily chosen parameter in the globally convergent Newton algorithm further underscores the robustness of the NCZ algorithm, for which convergence only depends on the right definition of Eq. (18) and Eq. (19).

Appendix H: Numerical test

https://doi.org/10.5194/tc-2020-293
Preprint. Discussion started: 19 October 2020

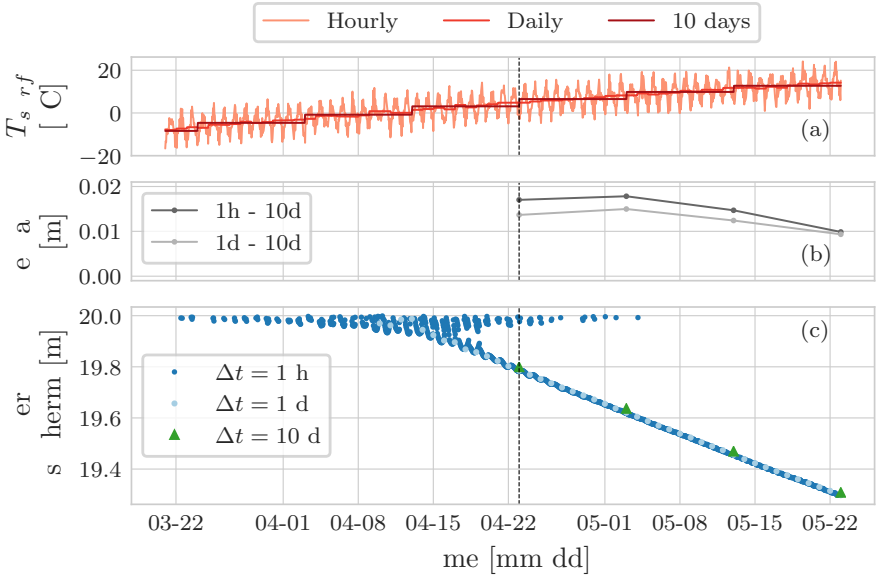

Figure H1. Detail of the beginning of the thawing season for the year 1999. In (b) there is a time lag of about one month between the beginning of thawing season for the hourly simulation and the 10-days one, dashed grey line. This can be attributed to the different surface temperature used to drive the simulations.

https://doi.org/10.5194/tc-2020-293
Preprint. Discussion started: 19 October 2020

The Cryosphere
Discussions
Open Access
EGU

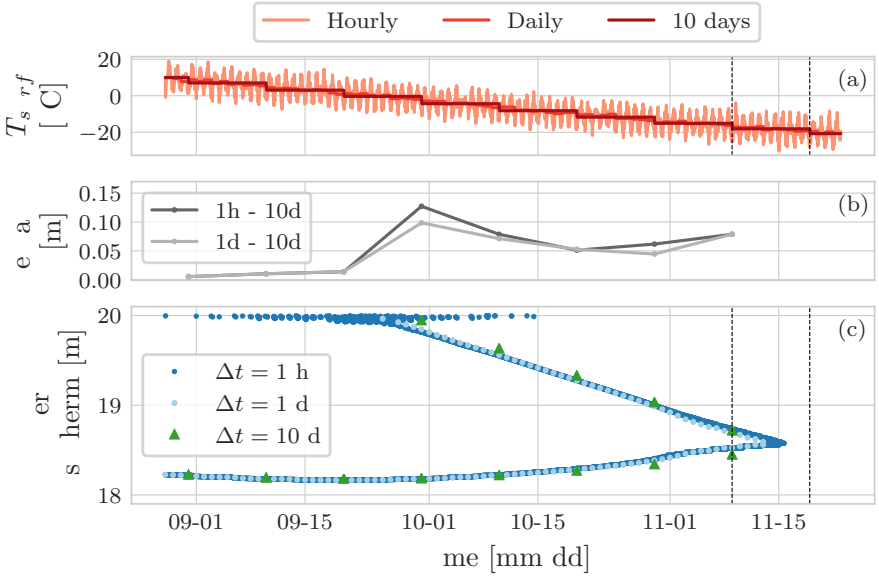

Figure H2. Detail of the freezing season for the year 1999. The joining of the downward and upward freezing front is captured by the hourly and the daily simulations, (c). It is interesting to note that for the 10 days simulation the joining occurs in-between of two consecutive time step.

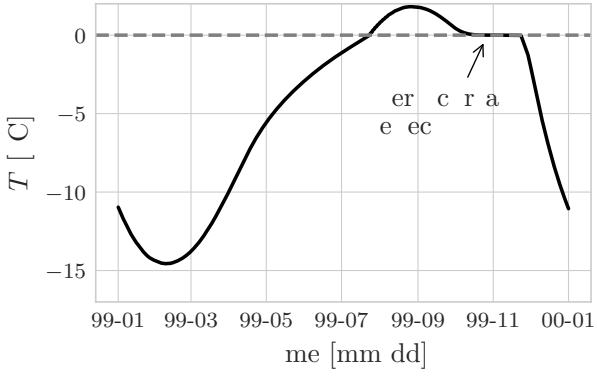

Figure H3. Hourly temperature at 1.5 m depth for the year 1999. Note the prolonged period (43 days, 11 October until 23 November) when temperature remained within ±0.1 °C (zero-curtain effect).

https://doi.org/10.5194/tc-2020-293
Preprint. Discussion started: 19 October 2020

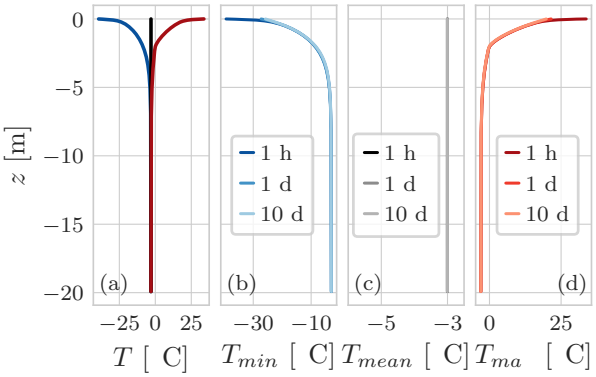

Figure H4. Temperature profile envelope for the three simulations considering $\lambda_w = \lambda_i$. In this case it is not possible to appreciate the typical 'trumpet profile'. The mean temperature is very close to the initial temperature profile, the maximum error is of 0.003 °C.

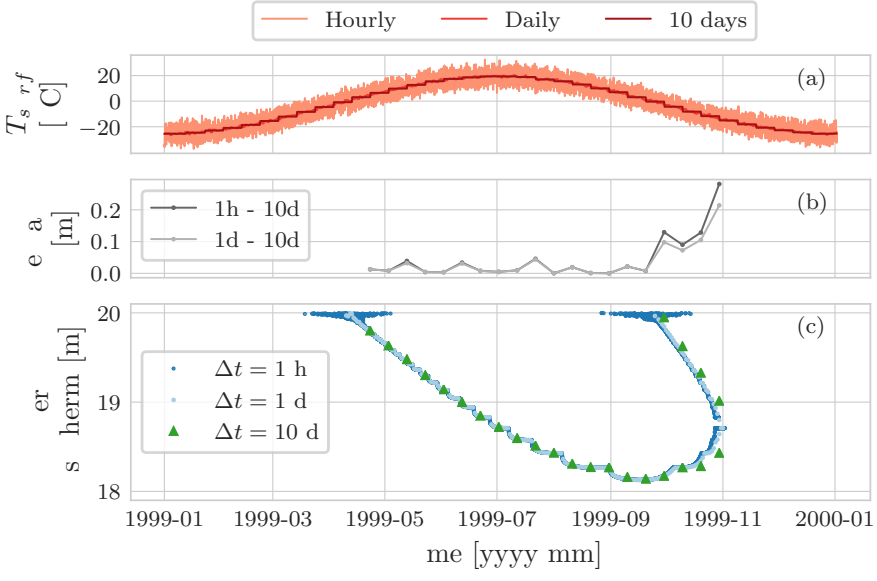

Figure H5. Comparison of the position of the zero-isotherm after 100 years of three simulations: one by using an hourly boundary condition with time step of $\Delta t = 1$ h, one by using a daily boundary condition with a time step of $\Delta t = 1$ day, and the last one by using a 10-days boundary condition with a time step of $\Delta t = 10$ day. The 'steps' are due to a coarser space discretization. Another consequence of this if that the joining of the downward and upward freezing front is not captured neither by the hourly and by the daily simulations.

https://doi.org/10.5194/tc-2020-293
Preprint. Discussion started: 19 October 2020

The Cryosphere Discussions
Open Access
EGU

Table H1. Input parameters for the comparison between Neumann analytical solution and the numerical solution.

Symbol	Parameter	Value	Units
Δt	time step	3600, 86400, 864000	s
Δz^a_{min}	thickness of the first control volume	0.002, 0.005	m
b^a	growth rate ground depth	0.01, 0.1	–
z_{max}	maximal ground depth	20	m
l_f	latent heat of fusion	333700	J kg^{-1}
c_w	specific heat of water	4188	J m^{-3} °C^{-1}
c_i	specific heat of ice	2117	J m^{-3} °C^{-1}
c_{sp}	specific heat of soil particles	1000	J m^{-3} °C^{-1}
ρ_w	water density	1000	kg m^{-3}
ρ_i	ice density	1000	kg m^{-3}
ρ_{sp}	soil particles density	2700	kg m^{-3}
λ_w	thermal conductivity of water	0.6	W m^{-1} °C^{-1}
λ_i	thermal conductivity of ice	2.09	W m^{-1} °C^{-1}
λ_{sp}	thermal conductivity of soil particles	3.0	W m^{-1} °C^{-1}
θ_s	saturation water content	0.46	–
θ_r	residual water content	0.1	–
α	Van Genuchten parameter	1.5	m^{-1}
n	Van Genuchten parameter	1.2	–
T_0	initial temperature	-3	°C
	SFCC	Dall'Amico	
	Thermal conductivity model	Johansen	

[a] We used two different space discretizations. The thickness of the ground layer is parametrized as $dz_i = dz_{min}(1+b)^{(i-1)}$ (Gubler et al., 2013).

https://doi.org/10.5194/tc-2020-293
Preprint. Discussion started: 19 October 2020

Author contributions. Conceptualization N.T., S.G., R.R; software N.T., R.R.; writing of original draft N.T.; reviewing and editing N.T., S.G., R.R. All the authors have read and agreed to the published version of the manuscript.

Competing interests. The authors declare no conflict of interest.

Acknowledgements. The first author would like to thank Professor Vincenzo Casulli and Professor Michael Dumbser of the Department of Civil, Environmental and Mechanics Engineering at the University of Trento for their fruitful discussions on the numerical aspects of the work. We thank Professor Andy Aschwanden, Professor Ed Bueler, and Professor Constantine Khrulev for their feedback regarding ice sheet models, and Dr. Samuel Morin for feedback regarding the model Crocus.

This work has been partially supported by a Ph.D. grant by the Department of Civil, Environmental and Mechanics Engineering at the University of Trento. In Canada, support was available through the NSERC Strategic Project "Improved Characterization of Permafrost Vulnerability to Support Decision Makers, Infrastructure, and Community Stewardship in the Northwest Territories" and NSERC PermafrostNet.

https://doi.org/10.5194/tc-2020-293
Preprint. Discussion started: 19 October 2020

References

Anderson, D. M. and Tice, A. R.: Predicting unfrozen water contents in frozen soils from surface area measurements, Highway research record, 393, 12–18, 1972.

Andreas, E. L. et al.: Handbook of physical constants and functions for use in atmospheric boundary layer studies, 2005.

Aschwanden, A. and Blatter, H.: Meltwater production due to strain heating in Storglaciären, Sweden, Journal of Geophysical Research: Earth Surface, 110, 2005.

Aschwanden, A. and Blatter, H.: Mathematical modeling and numerical simulation of polythermal glaciers, Journal of Geophysical Research: Earth Surface, 114, 2009.

Aschwanden, A., Bueler, E., Khroulev, C., and Blatter, H.: An enthalpy formulation for glaciers and ice sheets, Journal of Glaciology, 58, 441–457, 2012.

Bancheri, M.: A flexible approach to the estimation of water budgets and its connection to the travel time theory, Ph.D. thesis, University of Trento, 2017.

Bao, H., Koike, T., Yang, K., Wang, L., Shrestha, M., and Lawford, P.: Development of an enthalpy-based frozen soil model and its validation in a cold region in China, Journal of Geophysical Research: Atmospheres, 121, 5259–5280, 2016.

Bartelt, P. and Lehning, M.: A physical SNOWPACK model for the Swiss avalanche warning: Part I: numerical model, Cold Regions Science and Technology, 35, 123–145, 2002.

Boone, A. and Etchevers, P.: An intercomparison of three snow schemes of varying complexity coupled to the same land surface model: Local-scale evaluation at an Alpine site, Journal of Hydrometeorology, 2, 374–394, 2001.

Bouyoucos, G.: Degree of temperature to which soils can be cooled without freezing, Monthly Weather Review, 48, 718–718, 1920.

Bouyoucos, G. and McCool, M.: The freezing point method as a new means of measuring the concentration of the soil solution directly in the soil.• Mich, Agr. Exp. Sta. Tech. Bui, 24, 1915.

Bouyoucos, G. J.: An investigation of soil temperature and some of the most important facters influencing it, Technical Bulletin of Michigan Agriculture Experimental Station, 17, 1–196, 1913.

Bouyoucos, G. J.: Movement of soil moisture from small capillaries to the large capillaries of the soil upon freezing, Journal of Agricultural Research, 24, 427–432, 1923.

Brugnano, L. and Casulli, V.: Iterative solution of piecewise linear systems, SIAM Journal on Scientific Computing, 30, 463–472, 2008.

Brugnano, L. and Casulli, V.: Iterative solution of piecewise linear systems and applications to flows in porous media, SIAM Journal on Scientific Computing, 31, 1858–1873, 2009.

Brun, E., Martin, E., Simon, V., Gendre, C., and Coleou, C.: An energy and mass model of snow cover suitable for operational avalanche forecasting, Journal of glaciology, 35, 333–342, 1989.

Brun, E., David, P., Sudul, M., and Brunot, G.: A numerical model to simulate snow-cover stratigraphy for operational avalanche forecasting, Journal of Glaciology, 38, 13–22, 1992.

Callen, H. B.: Thermodynamics and an Introduction to Thermostatistics, John Wiley and Sons, Inc., 1985.

Casulli, V. and Walters, R. A.: An unstructured grid, three-dimensional model based on the shallow water equations, International Journal for Numerical Methods in Fluids, 32, 331–348, 2000.

Casulli, V. and Zanolli, P.: A nested Newton-type algorithm for finite volume methods solving Richards' equation in mixed form, SIAM Journal on Scientific Computing, 32, 2255–2273, 2010.

https://doi.org/10.5194/tc-2020-293
Preprint. Discussion started: 19 October 2020

Casulli, V. and Zanolli, P.: Iterative solutions of mildly nonlinear systems, Journal of Computational and Applied Mathematics, 236, 3937–3947, 2012.

Celia, M. A., Bouloutas, E. T., and Zarba, R. L.: A general mass-conservative numerical solution for the unsaturated flow equation, Water Resources Research, 26, 1483–1496, 1990.

Chistyakov, V.: On mappings of bounded variation, Journal of Dynamical and Control Systems, 3, 261, 1997.

Clow, G. D.: CVPM 1.1: a flexible heat-transfer modeling system for permafrost, Geoscientific Model Development, 11, 4889–4908, 2018.

Dai, Y., Zeng, X., Dickinson, R. E., Baker, I., Bonan, G. B., Bosilovich, M. G., Denning, A. S., Dirmeyer, P. A., Houser, P. R., Niu, G., et al.: The common land model, Bulletin of the American Meteorological Society, 84, 1013–1024, 2003.

Dall'Amico, M.: Coupled water and heat transfer in permafrost modeling, Ph.D. thesis, University of Trento, 2010.

Dall'Amico, M., Endrizzi, S., Gruber, S., and Rigon, R.: A robust and energy-conserving model of freezing variably-saturated soil, The Cryosphere, 5, 469–484, 2011.

D'Amboise, C. J., Müller, K., Oxarango, L., Morin, S., and Schuler, T.: Implementation of a physically based water percolation routine in the Crocus/SURFEX (V7. 3) snowpack model, Geoscientific Model Development, 10, 3547–3566, 2017.

David, O., Ascough II, J. C., Lloyd, W., Green, T. R., Rojas, K., Leavesley, G. H., and Ahuja, L. R.: A software engineering perspective on environmental modeling framework design: The Object Modeling System, Environmental Modelling & Software, 39, 201–213, 2013.

De Lorenzo, S., Di Renzo, V., Civetta, L., D'antonio, M., and Gasparini, P.: Thermal model of the Vesuvius magma chamber, Geophysical Research Letters, 33, 2006.

Endrizzi, S., Gruber, S., Dall'Amico, M., and Rigon, R.: GEOtop 2.0: simulating the combined energy and water balance at and below the land surface accounting for soil freezing, snow cover and terrain effects, Geoscientific Model Development, 7, 2831–2857, 2014.

Erum, J. V., Dam, D. V., and Deyn, P. P. D.: Parametrization of soil freezing characteristic curve for unsaturated soils, Cold Regions Science and Technology, https://doi.org/10.1016/j.neubiorev.2019.07.019, 2019.

Foley, J. A., Prentice, I. C., Ramankutty, N., Levis, S., Pollard, D., Sitch, S., and Haxeltine, A.: An integrated biosphere model of land surface processes, terrestrial carbon balance, and vegetation dynamics, Global Biogeochemical Cycles, 10, 603–628, 1996.

Formetta, G., Antonello, A., Franceschi, S., David, O., and Rigon, R.: Hydrological modelling with components: A GIS-based open-source framework, Environmental Modelling & Software, 55, 190–200, 2014.

Goodrich, L.: Some results of a numerical study of ground thermal regimes, in: Proceedings of the Third International Conference on Permafrost, National Research Council of Canada, Ottawa, Edmonton, Canada, 1978.

Goodrich, L.: The influence of snow cover on the ground thermal regime, Canadian Geotechnical Journal, 19, 421–432, 1982.

Greve, R.: Application of a polythermal three-dimensional ice sheet model to the Greenland ice sheet: response to steady-state and transient climate scenarios, Journal of Climate, 10, 901–918, 1997a.

Greve, R.: A continuum–mechanical formulation for shallow polythermal ice sheets, Philosophical Transactions of the Royal Society of London. Series A: Mathematical, Physical and Engineering Sciences, 355, 921–974, 1997b.

Greve, R. and Blatter, H.: Comparison of thermodynamics solvers in the polythermal ice sheet model SICOPOLIS, Polar Science, 10, 11–23, 2016.

Gubler, S., Endrizzi, S., Gruber, S., and Purves, R. S.: Sensitivities and uncertainties of modeled ground temperatures in mountain environments, Geoscientific Model Development, 6, 1319–1336, 2013.

Hansson, K., Šimünek, J., Mizoguchi, M., Lundin, L.-C., and Van Genuchten, M. T.: Water flow and heat transport in frozen soil, Vadose Zone Journal, 3, 693–704, 2004.

https://doi.org/10.5194/tc-2020-293
Preprint. Discussion started: 19 October 2020

Harris, C., Arenson, L. U., Christiansen, H. H., Etzelmüller, B., Frauenfelder, R., Gruber, S., Haeberli, W., Hauck, C., Hoelzle, M., Humlum, O., et al.: Permafrost and climate in Europe: Monitoring and modelling thermal, geomorphological and geotechnical responses, Earth-Science Reviews, 92, 117–171, 2009.

Hollesen, J., Elberling, B., and Jansson, P.-E.: Future active layer dynamics and carbon dioxide production from thawing permafrost layers in Northeast Greenland, Global Change Biology, 17, 911–926, 2011.

Hu, H. and Argyropoulos, S. A.: Mathematical modelling of solidification and melting: a review, Modelling and Simulation in Materials Science and Engineering, 4, 371, 1996.

InterFrost Project: https://wiki.lsce.ipsl.fr/interfrost/doku.php?id=test_cases:one, accessed: 20/08/2020.

Jansson, P. and Karlberg, L.: Coupled heat and mass transfer model for soil-plant-atmosphere systems, Royal Institute of Technology, Dept of Civil and Environmental Engineering, Stockholm, 2011.

Kozlowski, T.: A semi-empirical model for phase composition of water in clay–water systems, Cold Regions Science and Technology, 49, 226–236, 2007.

Kurylyk, B. L. and Watanabe, K.: The mathematical representation of freezing and thawing processes in variably-saturated, non-deformable soils, Advances in Water Resources, 60, 160–177, 2013.

Kurylyk, B. L., MacQuarrie, K. T., and McKenzie, J. M.: Climate change impacts on groundwater and soil temperatures in cold and temperate regions: Implications, mathematical theory, and emerging simulation tools, Earth-Science Reviews, 138, 313–334, 2014a.

Kurylyk, B. L., McKenzie, J. M., MacQuarrie, K. T., and Voss, C. I.: Analytical solutions for benchmarking cold regions subsurface water flow and energy transport models: One-dimensional soil thaw with conduction and advection, Advances in Water Resources, 70, 172–184, 2014b.

Langham, E.: Phase equilibria of veins in polycrystalline ice, Canadian Journal of Earth Sciences, 11, 1280–1287, 1974.

Lawrence, D., Fisher, R., Koven, C., Oleson, K., Swenson, S., and Vertenstein, M.: CLM5 documentation, Tech. rep., Tech. rep., Boulder, CO: National Center for Atmospheric Research, 2019.

Lehning, M., Bartelt, P., Brown, B., Russi, T., Stöckli, U., and Zimmerli, M.: SNOWPACK model calculations for avalanche warning based upon a new network of weather and snow stations, Cold Regions Science and Technology, 30, 145–157, 1999.

Lewis, R. and Ravindran, K.: Finite element simulation of metal casting, International journal for numerical methods in engineering, 47, 29–59, 2000.

Lliboutry, L. and Duval, P.: Various isotropic and anisotropic ices found in glaciers and polar ice caps and their corresponding rheologies, in: Annales Geophysicae, vol. 3, pp. 207–224, 1985.

Lunardini, V. J.: Freezing of soil with an unfrozen water content and variable thermal properties, Tech. Rep. 88-2, US Army Corps of Engineers, Cold Regions Research & Engineering Laboratory, 1988.

Marchenko, S., Romanovsky, V., and Tipenko, G.: Numerical modeling of spatial permafrost dynamics in Alaska, in: Proceedings of the ninth international conference on permafrost, vol. 29, pp. 1125–1130, Institute of Northern Engineering, University of Alaska Fairbanks, 2008.

McKenzie, J. M. and Voss, C. I.: Permafrost thaw in a nested groundwater-flow system, Hydrogeology Journal, 21, 299–316, 2013.

McKenzie, J. M., Voss, C. I., and Siegel, D. I.: Groundwater flow with energy transport and water–ice phase change: numerical simulations, benchmarks, and application to freezing in peat bogs, Advances in Water Resources, 30, 966–983, 2007.

Mongibello, L., Bianco, N., Caliano, M., and Graditi, G.: Numerical simulation of an aluminum container including a phase change material for cooling energy storage, Applied System Innovation, 1, 34, 2018.

https://doi.org/10.5194/tc-2020-293
Preprint. Discussion started: 19 October 2020

Nazzi Ehms, J. H., De Césaro Oliveski, R., Oliveira Rocha, L. A., Biserni, C., and Garai, M.: Fixed grid numerical models for solidification and melting of phase change materials (PCMs), Applied Sciences, 9, 4334, 2019.

Nedjar, B.: An enthalpy-based finite element method for nonlinear heat problems involving phase change, Computers & Structures, 80, 9–21, 2002.

Nicolsky, D., Romanovsky, V., Alexeev, V., and Lawrence, D.: Improved modeling of permafrost dynamics in a GCM land-surface scheme, Geophysical Research Letters, 34, 2007a.

Nicolsky, D., Romanovsky, V., and Tipenko, G.: Using in-situ temperature measurements to estimate saturated soil thermal properties by solving a sequence of optimization problems, The Cryosphere, 1, 41–58, 2007b.

Oleson, K., Dai, Y., Bonan, B., Bosilovichm, M., Dickinson, R., Dirmeyer, P., Hoffman, F., Houser, P., Levis, S., Niu, G.-Y., et al.: Technical description of the Community Land Model (CLM), Tech. rep., NCAR, 2004.

Painter, S. L.: Three-phase numerical model of water migration in partially frozen geological media: model formulation, validation, and applications, Computational Geosciences, 15, 69–85, 2011.

Paniconi, C. and Putti, M.: A comparison of Picard and Newton iteration in the numerical solution of multidimensional variably saturated flow problems, Water Resources Research, 30, 3357–3374, 1994.

Rempel, A. W., Wettlaufer, J., and Worster, M. G.: Premelting dynamics in a continuum model of frost heave, Journal of Fluid Mechanics, 498, 227, 2004.

Rigon, R., Bertoldi, G., and Over, T. M.: GEOtop: A distributed hydrological model with coupled water and energy budgets, Journal of Hydrometeorology, 7, 371–388, 2006.

Riseborough, D., Shiklomanov, N., Etzelmüller, B., Gruber, S., and Marchenko, S.: Recent advances in permafrost modelling, Permafrost and Periglacial Processes, 19, 137–156, 2008.

Roe, P. L.: Approximate Riemann solvers, parameter vectors, and difference schemes, Journal of Computational Physics, 43, 357–372, 1981.

Ruhaak, W., Anbergen, H., Grenier, C., McKenzie, J., Kurylyk, B., Molson, J., Roux, N., and Sass, I.: Benchmarking numerical freeze/thaw models, Energy Procedia, 2015.

Schuur, E. A., McGuire, A. D., Schädel, C., Grosse, G., Harden, J., Hayes, D. J., Hugelius, G., Koven, C. D., Kuhry, P., Lawrence, D. M., et al.: Climate change and the permafrost carbon feedback, Nature, 520, 171–179, 2015.

Sergueev, D., Tipenko, G., Romanovsky, V., and Romanovskii, N.: Mountain permafrost thickness evolution under influence of long-term climate fluctuations (results of numerical simulation), in: Proceedings of the VII International Permafrost Conference, Switzerland, pp. 21–25, 2003.

Sheshukov, A. Y. and Nieber, J. L.: One-dimensional freezing of nonheaving unsaturated soils: Model formulation and similarity solution, Water Resources Research, 47, 2011.

Shewchuk, J. R.: An Introduction to the Conjugate Gradient Method Without the Agonizing Pain, Tech. rep., USA, 1994.

Streletskiy, D. A., Suter, L. J., Shiklomanov, N. I., Porfiriev, B. N., and Eliseev, D. O.: Assessment of climate change impacts on buildings, structures and infrastructure in the Russian regions on permafrost, Environmental Research Letters, 14, 025 003, 2019.

Tan, X., Chen, W., Tian, H., and Cao, J.: Water flow and heat transport including ice/water phase change in porous media: numerical simulation and application, Cold Regions Science and Technology, 68, 74–84, 2011.

Tubini, N.: https://zenodo.org/record/4017668#.X4l3f-1S82w, last accessed: 16 October 2020, a.

Tubini, N.: OMS project, https://github.com/GEOframeOMSProjects/OMS_FreeThaw1D, last accessed: 16 October 2020, b.

Tubini, N.: source code, https://github.com/geoframecomponents/FreeThaw1D, last accessed: 16 October 2020, c.

https://doi.org/10.5194/tc-2020-293
Preprint. Discussion started: 19 October 2020

Verseghy, D. L.: CLASS—A Canadian land surface scheme for GCMs. I. Soil model, International Journal of Climatology, 11, 111–133, 1991.

Vionnet, V., Brun, E., Morin, S., Boone, A., Faroux, S., Le Moigne, P., Martin, E., and Willemet, J.: The detailed snowpack scheme Crocus and its implementation in SURFEX v7. 2, 2012.

Voller, V. and Cross, M.: Accurate solutions of moving boundary problems using the enthalpy method, International Journal of Heat and Mass Transfer, 24, 545–556, 1981.

Voller, V. R.: Fast implicit finite-difference method for the analysis of phase change problems, Numerical Heat Transfer, 17, 155–169, 1990.

Voller, V. R., Swaminathan, C., and Thomas, B. G.: Fixed grid techniques for phase change problems: a review, International Journal for Numerical Methods in Engineering, 30, 875–898, 1990.

Voss, C. I. and Provost, A.: SUTRA: A model for 2D or 3D saturated-unsaturated, variable-density ground-water flow with solute or energy transport, Tech. rep., U.S. Geological Survey Water-Resources Investigations Report, 2002.

Vuik, C.: Some historical notes about the Stefan problem, 1993.

Walvoord, M. A. and Kurylyk, B. L.: Hydrologic impacts of thawing permafrost—A review, Vadose Zone Journal, 15, 2016.

Watanabe, K. and Mizoguchi, M.: Amount of unfrozen water in frozen porous media saturated with solution, Cold Regions Science and Technology, 34, 103–110, 2002.

Watanabe, K., Kito, T., Wake, T., and Sakai, M.: Freezing experiments on unsaturated sand, loam and silt loam, Annals of Glaciology, 52, 37–43, 2011.

Westermann, S., Schuler, T., Gisnås, K., and Etzelmüller, B.: Transient thermal modeling of permafrost conditions in Southern Norway, The Cryosphere, 7, 719–739, 2013.

Westermann, S., Langer, M., Boike, J., Heikenfeld, M., Peter, M., Etzelmüller, B., and Krinner, G.: Simulating the thermal regime and thaw processes of ice-rich permafrost ground with the land-surface model CryoGrid 3, Geoscientific Model Development, 9, 523–546, 2016.

Zhang, Y., Chen, W., and Cihlar, J.: A process-based model for quantifying the impact of climate change on permafrost thermal regimes, Journal of Geophysical Research: Atmospheres, 108, 2003.

Zhang, Y., Carey, S. K., and Quinton, W. L.: Evaluation of the algorithms and parameterizations for ground thawing and freezing simulation in permafrost regions, Journal of Geophysical Research: Atmospheres, 113, 2008.